Pergamon

Geochimica et Cosmochimica Acta, Vol. 68, No. 20, pp. 4249-4266, 2004

0016-7037/04 $30.00 + .00

doi:10.1016/j.gca.2004.01.027

Feldspathic clast populations in polymict ureilites: Stalking the missing basalts from the ureilite parent body

BARBARA A. COHEN,* CYRENA A. GOODRICH,† and KLAUS KEIL

Hawaii Institute of Geophysics and Planetology, School of Ocean and Earth Sciences and Technology, University of Hawaii at Manoa, Honolulu, HI 96822, USA

(Received July 28, 2003; *accepted in revised form January* 21, 2004)

Abstract—Polymict ureilites DaG 164/165, DaG 319, DaG 665, and EET 83309 are regolith breccias composed mainly of monomict ureilite-like material, but containing ~2 vol% of feldspathic components. We characterized 171 feldspathic clasts in these meteorites in terms of texture, mineralogy, and mineral compositions. Based on this characterization we identified three populations of clasts, each of which appears to represent a common igneous (generally basaltic) lithology and whose mafic minerals show a normal igneous fractionation trend of near-constant Fe/Mn ratio over a range of Fe/Mg ratios that extend to much higher values than those in monomict ureilites. The melts represented by these populations are unlikely to be impact melts, because the ubiquitous presence of carbon in polymict ureilites (the regolith of the ureilite parent body) implies that impact melts would have crystallized under conditions of carbon redox control and therefore have highly magnesian mafic mineral compositions with constant Mn/Mg ratio. Therefore, these melts appear to be indigenous products of igneous differentiation on the ureilite parent body (UPB), complementary to the olivine-pigeonite residues represented by the majority of monomict ureilites.

The most abundant population is characterized by albitic plagioclase in association with pyroxenes, phosphates, ilmenite, silica, and incompatible-element enriched glass. Model calculations suggest that it formed by extensive fractional crystallization of the earliest melt(s) of precursor materials from which the most magnesian (shallowest) olivine-pigeonite ureilites formed. A less abundant population, characterized by labradoritic plagioclase, may have formed from melts complementary to more ferroan olivine-pigeonite ureilites, and derived from deeper in the UPB. The third population, characterized by the presence of olivine and augite, could only have formed from melts produced at greater depths in the UPB than the olivine-pigeonite ureilites. Many other feldspathic clasts cannot be positively associated with any of these three populations, because their mafic mineral compositions exhibit carbon redox control. However, they may be products of early crystallization of basaltic melts produced on the UPB, before carbon was exhausted by reduction.

Partial melting on the ureilite parent body was a fractional (or incremental) process. Melts were produced early in UPB history, and most likely extracted rapidly, thus preserving primitive chemical and oxygen isotopic signatures in the residues. *Copyright © 2004 Elsevier Ltd*

1. INTRODUCTION

Ureilites are the second-largest group of achondritic meteorites. They are ultramafic rocks composed mainly of magnesian (mg# [100 × molar Mg/(Mg + Fe)] = 76 to 95) olivine and pyroxene (dominantly pigeonite), with minor carbon-phases, metal, and sulfide (Goodrich, 1992; Mittlefehldt et al., 1998). They are coarse-grained, slowly cooled, and depleted in incompatible lithophile and plagiophile elements, suggesting their origin as igneous rocks. In contrast to these igneous properties, they appear to preserve primitive features, such as O-isotopic compositions ranging along a $\delta^{17}O$-$\delta^{18}O$ line with slope ~1, high abundances of noble gases, and constant, near-chondritic MnO/MgO ratio over a large range in FeO/MgO ratios. Thus, monomict ureilites are thought to be residues of partial melting on an asteroidal parent body that experienced only a limited degree of igneous processing. Rapid extraction of partial melts from a range of depths could leave intact the range of primitive signatures seen among the residues, and explain the lack of igneous fractionation trends among them. Their large range of FeO/MgO ratios is thought to be due to carbon redox control (smelting) over a range of pressures (Berkley and Jones, 1982; Goodrich et al., 1987; Warren and Kallemeyn, 1992; Walker and Grove, 1993; Sinha et al., 1997; Singletary and Grove, 2003a), rather than to different degrees of melting. ~25%–30% partial melting of chondritic-like precursor materials could produce olivine-pyroxene residues similar to the monomict ureilitic ureilites, although those precursors must have been enriched in Ca relative to Al to produce pigeonite rather than orthopyroxene (Goodrich, 1999).

Partial melting of such precursors would also have produced basaltic material enriched in incompatible elements. However, basaltic meteorites complementary to the ultramafic monomict ureilites are unknown in the meteorite collection. The composition of this basaltic component would provide compositional, isotopic, and geochronologic information critical to constraining the bulk composition and evolution of the ureilite parent body (UPB).

Feldspathic (plagioclase-bearing) clasts occur as a minor component in some polymict ureilites, which are regolith and

* Author to whom correspondence should be addressed, at Department of Earth and Planetary Sciences, University of New Mexico, Albuquerque, NM 87131, USA (bcohen@unm.edu).
† *Present address:* Department of Physical Sciences, Kingsborough Community College, 2001 Oriental Avenue, Brooklyn, NY 11209, USA.

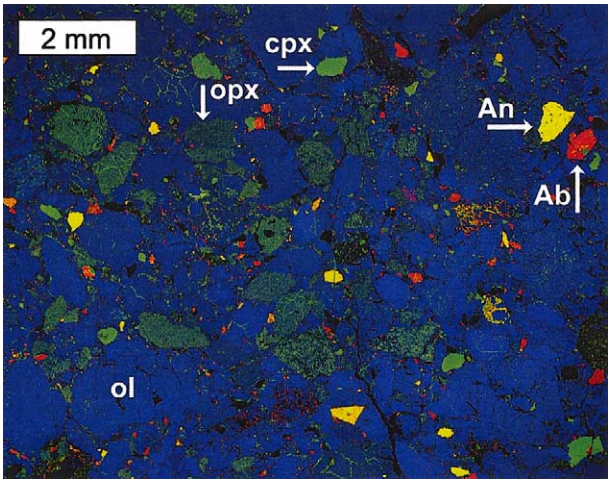

Fig. 1. Three-element X-ray map (red = Al, green = Ca, blue = Mg) of part of the DaG 164 thin section, showing the abundance and distribution of feldspathic clasts. In this representation, olivine (ol) is blue, pyroxene has a range of green tones with increasing Ca content from dull green for orthopyroxene (opx) to bright green for Ca-rich pyroxene (cpx), and feldspar shows a range of red tones with increasing Ca content from red in albite (Ab) to yellow in anorthite (An). Feldspathic clasts make up ≤2% by volume in polymict ureilites.

near-surface breccias composed predominantly of clasts of monomict ureilitic material. Feldspathic clasts have been identified in Nilpena, North Haig, Dar al Gani (DaG) 165, DaG 319, DaG 665, and Elephant Moraine (EET) 83309 (Prinz et al., 1986, 1987; Warren and Kallemeyn, 1989; Warren and Kallemeyn, 1991; Ikeda et al., 2000; Guan and Crozaz, 2001; Ikeda and Prinz, 2001; Goodrich and Keil, 2002). The oxygen-isotope compositions of a diverse set of feldspathic clasts found in DaG 319 and EET 83309 plot along the ureilite mixing line (slope ~1) with $\delta^{17}O$ values similar to those in monomict ureilites (Kita et al., 2000; Guan and Leshin, 2001). Thus, it seems probable that many feldspathic clasts in the polymict ureilites are pieces of basaltic lithologies created during igneous evolution of the UPB.

Because these clasts typically constitute ≤2% by volume of polymict ureilites, and are smaller than 500 μm in size, descriptions and analyses of them are sparse and have largely been unrelated to one another. It is likely that any given clast is not representative of the complete mineral assemblage of the rock from which it is derived, necessitating the discovery of many related clasts to adequately characterize the lithology. If feldspathic clasts do indeed hold clues to the missing ureilitic basalts, they deserve a thorough treatment.

We conducted a search for and characterization of feldspathic clasts >80 μm in size in thin sections of seven polymict ureilites: DaG 164, DaG 165, DaG 319, DaG 665, EET 83309, EET 96001, and Frontier Mountain (FRO) 93008. Our principal goal was to identify populations of clasts representing pristine basaltic lithologies (as opposed to nonindigenous material or impact melts) from the UPB. In this paper, we characterize the populations that were identified, based on chemical and textural properties of 171 clasts. We then investigate the possible origin of several of these populations, and discuss criteria for distinguishing whether clasts are derived from primary (pristine) igneous rocks or from secondary processes such as impact. These criteria for pristinity differ from those that can be applied to breccias of other meteorite types, due to unique properties of the UPB. For those populations that appear likely to represent pristine basaltic lithologies, we model possible relationships to monomict ureilites, and discuss the implications of the results for the differentiation history of the UPB.

2. METEORITES AND TECHNIQUES

The four Dar al Gani meteorites in this study were recovered in the Libyan Sahara. DaG 164 and DaG 165 were found in 1996. The two recovered pieces of DaG 164 weigh a total of 57 g; one recovered piece of DaG 165 weighs 32 g. Both were only moderately shocked (shock stage S3) and both have been moderately terrestrially weathered (Grossman, 1997). DaG 319 was found in three pieces in 1997, weighing a combined 740 g. It experienced only mild shock and terrestrial weathering compared with DaG 164/165 (Grossman, 1998). DaG 164 and 165 are almost certainly paired, and preliminary examinations suggest that DaG 319 may be paired with them as well. All three meteorites are microbreccias containing lithic clasts up to 1 cm across, mineral clasts up to 1 mm across, and several different kinds of other clasts (e.g., sulfides, metal, dark inclusions, chondritic material; Grossman, 1998; Ikeda et al., 2000; Ikeda and Prinz, 2001). Lithic clasts consist predominantly of material similar to monomict ureilites, but several vol% of the lithic fragments contain a feldspathic component.

DaG 665 was recovered as a single 363-g stone in 1999. It is a fragmental breccia with lithic and mineral clasts embedded in a cataclastic matrix (Grossman and Zipfel, 2001). Lithic clasts are dominantly material similar to monomict ureilites, with

Table 1. Characteristics of thin sections studied.

Meteorite	Section area (cm^2)	No. of feldspathic clasts identified	Feldspathic clasts (vol%)	Clast designations	Size range of clasts (μm)
DaG 164	1.88	29	2	C1-C31	100–1000
DaG 165	1.28	32	2	4-36	100–800
DaG 319	4.60	37	2	B1-B38	40–1000
DaG 665	1.14	51	6[a]	E1-E51	100–6000
EET 83309,3	0.50	22	1.5	D1-D22	50–300
EET 96001,08 and,13	0.36, 0.09	0	0	—	—
FRO 93008	0.23	0	0	—	—

[a] Including two 2-cm feldspathic clasts; ~2% without these clasts.

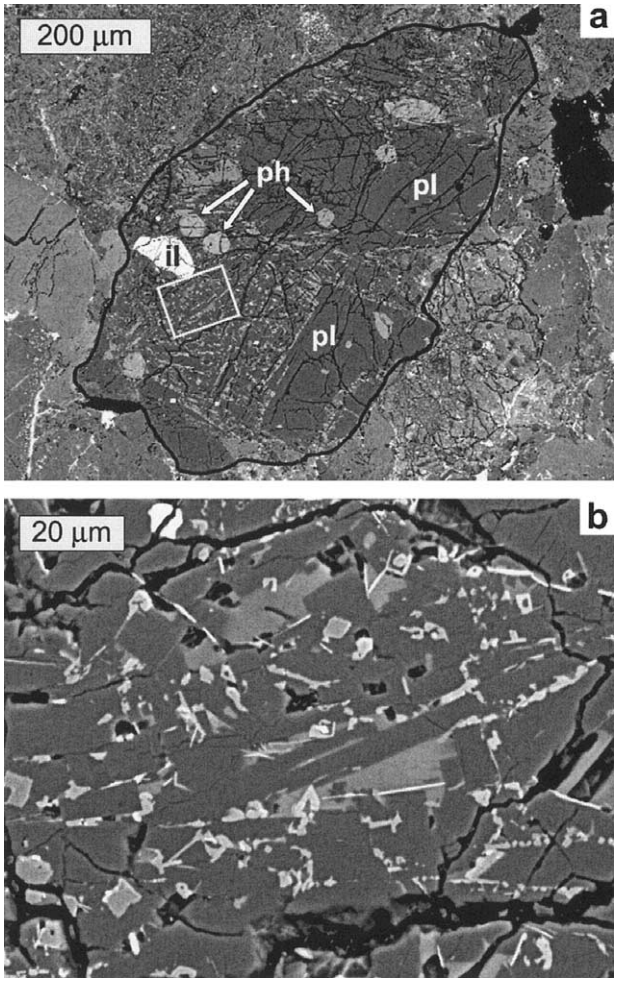

Fig. 2. Backscattered electron images of DaG 165 Clast 9, an albitic clast. (a) Clast is outlined in black and comprises large plagioclase (pl) crystals, interstitial areas of intersertal texture and rounded phosphate (ph) and ilmenite (il) grains. (b) Close-up of intersertal-textured area outlined in white box in (a). Dark gray laths are plagioclase, medium-gray areas are glassy mesostasis, light gray is pyroxene, and white needles are ilmenite.

Table 2. Representative mineral analyses in DaG 164 Clast 9, an albitic clast.[a]

Oxide (wt%)	Pyroxene	Plagioclase	Apatite	Whitlockite	Ilmenite
SiO_2	50.62	67.23	0.48	0.77	0.01
TiO_2	1.5	0.1	n.d.	n.d.	55.6
Al_2O_3	1.14	19.69	n.d.	0.11	0.06
Cr_2O_3	0.5	n.d.	n.d.	n.d.	1.6
FeO	15.48	0.10	1.17	1.93	37.73
MnO	1.09	n.d.	0.20	0.12	1.19
MgO	14.71	0.02	0.35	3.08	3.84
CaO	12.93	1.10	50.10	44.03	0.06
Na_2O	0.59	10.59	0.54	2.29	n.a.
K_2O	n.a.	0.6	n.d.	n.d.	n.a.
P_2O_5	n.a.	n.d.	41.4	52.8	n.a.
Cl	n.a.	n.a.	2.6	n.d.	n.a.
Total	98.48	99.47	96.79	105.08	100.06
Cations	(O_6)	(O_8)	(O_{12})	(O_8)	(O_3)
Si	1.94	2.96	0.04	0.05	—
Ti	0.04	0.00	0.00	0.00	1.01
Al	0.05	1.02	0.00	0.01	0.00
Cr	0.01	—	—	—	0.03
Fe	0.50	0.00	0.08	0.08	0.76
Mn	0.04	0.00	0.01	0.00	0.02
Mg	0.84	0.00	0.04	0.22	0.14
Ca	0.53	0.05	4.39	2.23	0.00
Na	0.04	0.90	0.09	0.21	—
K	—	0.04	0.00	0.00	—
P	—	—	2.86	2.11	—
Cl	—	—	0.18	0.00	—
Total	4.00	4.99	7.70	4.92	1.97
Wo	28.4				
En	45.0				
mg#	62.9				
An		5.23			
Ab		91.1			

[a] n.a. = not analyzed; n.d. = not detected.

minor components of feldspathic material and dark objects. It may be paired with DaG 319 (Grossman, 1998; Ikeda et al., 2000).

EET 83309, the only Antarctic meteorite in this study containing feldspathic clasts, is a heterogeneous microbreccia consisting of mineral clasts up to 3 mm and lithic clasts up to 1 mm in size, set into a black (C-rich) matrix strewn with small mineral clasts (Prinz et al., 1987). In terms of bulk composition, it is indistinguishable from monomict ureilites except in having high concentrations of La, Sm, and Eu (Warren and Kallemeyn, 1989) that are probably due to the presence of feldspathic clasts.

We also studied Antarctic meteorites FRO 93008 and EET 96001. EET 96001 (Satterwhite and Lindstrom, 1998) is a very fine-grained microbreccia of olivine clasts (up to 1.2 mm in size) with minor plagioclase and polysynthetically twinned pyroxene in a black matrix. Traces of nickel-iron and troilite are present along grain boundaries. We investigated two sections of this meteorite (EET 96001,08 and, 13) but found no evidence of feldspathic material in either section. FRO 93008 is compositionally heterogeneous over the scale of a thin section; one section contains two distinct, coarse-grained lithologies (olivine-pigeonite and olivine-augite-pigeonite) in contact with each other along a thin, cataclastic zone (Smith et al., 2000; Fioretti and Goodrich, 2001). Most of the clasts along the contacts are derived from the adjacent lithologies, but clasts of nonureilitic olivine, orthopyroxene, and feldspathic glass are also present (Fioretti and Goodrich, 2001). We investigated these clasts further, but found no multi-phase feldspathic clasts.

Each thin section was mapped in Al, Ca, and Mg Kα X-rays using a CAMECA SX-50 electron microprobe, scanning across the stage in 10-μm steps at 100 nA beam current. The three X-ray element maps were combined using the multispectral image-processing program ENVI (Hicks et al., 2002). The resulting maps permitted easy identification of feldspathic clasts $>$50 μm (Fig. 1). Individual clast textures were investigated using a JEOL JSM-5900 scanning electron microscope. Compositional data for mineral phases was obtained with the microprobe using mineral and synthetic standards. Operating currents of 15–20 nA and a focused electron beam were used for feldspar, pyroxene, olivine, and other mineral phases. Each element was counted for 20 s, except Na, which was counted for 10 s as the first element in the sequence. Glass phases were

analyzed using glass standards, beam currents of 5–10 nA, and beam sizes ≥5 μm. Both mineral and glass analyses were corrected using standard PAP corrections (Pouchou and Pichoir, 1985). Bulk compositions were determined by averaging analyses made using beam currents of 15–20 nA and a defocused (10–15 μm) beam, and were uncorrected beyond the PAP correction of individual analyses.

We studied in detail 32 feldspathic clasts in DaG 165 (clasts numbered 4–36), 37 in DaG 319 (B1-B38), 29 in DaG 164 (C1-C31), 22 in EET 83309 (D1-D22) and 51 in DaG 665 (E1-E51). Table 1 lists some of the characteristics of feldspathic clasts in each meteorite.

3. FELDSPATHIC CLAST POPULATIONS

Among the 171 clasts studied, we are able to identify several distinct populations of feldspathic clasts. In the following subsections, we present the characteristics of each population, including textures, mineral compositions, and mineral compositional trends. Consideration of criteria for pristinity suggests that at least three of these populations represent primary ureilitic melts, and so for these we examine possible petrogenetic relationships to monomict ureilites. Previous studies (Ikeda et al., 2000; Guan and Crozaz, 2001; Ikeda and Prinz, 2001) have described a number of feldspathic clasts in DaG 319 and EET 83309. To the extent we are able, we identify the clasts from those studies that belong to our populations, based on mineralogy and texture.

3.1. Albitic Clasts

The most common feldspathic clasts are characterized by albitic ($Ab_{75–99}$) plagioclase in association with one or more of a diverse assemblage of minerals. We have identified 54 lithic clasts that belong to this lithology, occurring in all five meteorites. Most of these clasts have irregular, sometimes angular shapes, suggesting that they are fragments of a larger body of rock (rather than each clast being an individually-produced rock such as an impact melt droplet). Two representative multiphase clasts are shown in Figures 2 and 3, with their mineralogy given in Tables 2 and 3. The ranges of all plagioclase and pyroxene compositions in this population are shown in Figure 4.

The most complete phase assemblage consists of plagioclase, pyroxene, phosphates, ilmenite, silica, and glass. Phenocrysts (up to 100 μm) of albitic plagioclase occur as large grains, which are often single crystals. Pyroxene is FeO-rich (Fig. 4) and occurs both as subhedral grains and as skeletal crystals; larger grains are normally zoned. Apatite and whitlockite can both occur in the same clast; phosphates are usually rounded and occur in a variety of sizes, sometimes enclosed within plagioclase grains. Ilmenite is found as small grains, and in a few clasts, as needles in a glass phase (Fig. 3). The glass occurs as coherent patches (e.g., Fig. 3b), and is rich in FeO (molar Fe/Mg = 11–18), K_2O (up to 4%), P_2O_5 (up to ~2%) and, except for where ilmenite needles have formed, TiO_2 (up to ~2.5%) (Table 3). A silica phase occurs as small, blocky crystals in the glass, sometimes lining ilmenite needles.

Often, the clasts contain areas with a distinct intersertal texture, in which fine-grained (2 μm) plagioclase laths (com-

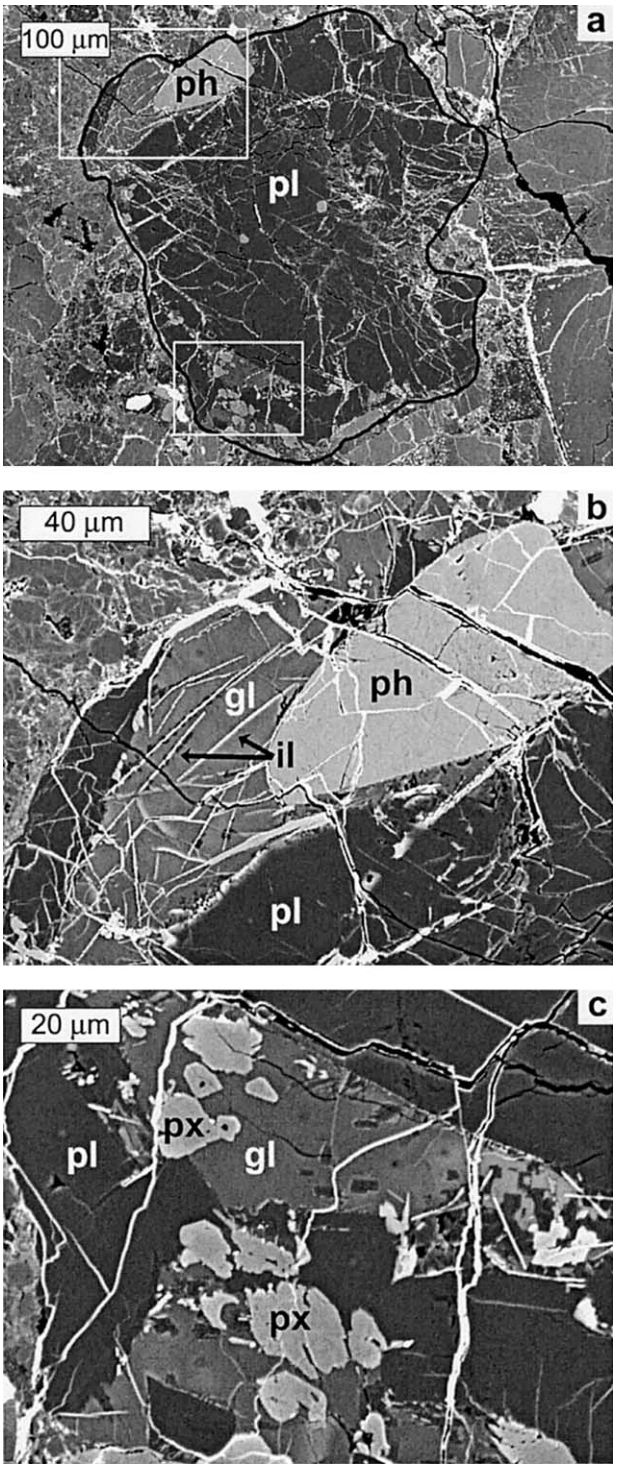

Fig. 3. Backscattered electron images of DaG 319 Clast B1, an albitic clast. (a) Clast is outlined in black. It is mostly crystalline plagioclase (pl) with rounded phosphate grains (ph) and glassy areas (gl). White boxes show enlarged views: (b) ilmenite needles (il) in glass; (c) glass and anhedral pyroxene grains (px) with a range of compositions. Silica appears as small, dark, blocky grains in glass phases along ilmenite needles in (b) and (c).

Table 3. Representative mineral analyses and average glass analyses in DaG 319 Clast B1, an albitic clast.[a]

Oxide (wt%)	Low-mg Pyroxene	High-mg Pyroxene	Plagioclase	Apatite	Oxide (wt%)	Glass (b)	Glass (c)
	50.97	50.62	66.65	0.08			
SiO_2					SiO_2	69.20	71.65
TiO_2	0.5	1.5	0.1	n.d.	TiO_2	1.2	2.1
Al_2O3	0.22	0.75	20.73	n.d.	Al_2O3	7.24	10.05
Cr_2O_3	0.3	0.7	n.d.	n.d.	Cr_2O_3	n.d.	n.d.
FeO	23.27	14.55	0.29	1.89	FeO	11.81	7.50
MnO	1.45	1.02	0.04	0.16	MnO	0.53	0.31
MgO	17.41	14.80	0.02	3.10	MgO	0.33	0.20
CaO	4.38	14.11	1.19	46.00	CaO	0.60	0.28
Na_2O	0.17	0.59	10.38	2.28	Na_2O	3.22	3.61
K_2O	n.d.	n.d.	0.6	n.d.	K_2O	3.8	3.2
P_2O_5	n.d.	0.1	0.1	46.0	P_2O_5	1.0	0.7
Total	98.69	98.77	100.09	99.53	Total	98.93	99.56
Cations	(O_6)	(O_6)	(O_8)	(O_{12})	Normative mineralogy (vol%)		
Si	1.97	1.94	2.92	0.01	Quartz	34.9	34.7
Ti	0.01	0.04	0.00	—	Na_2SiO_3	3.06	0.00
Al	0.01	0.03	1.07	—	Hypersthene	15.8	8.17
Cr	0.01	0.02	0.00	—	Albite	17.8	32.5
Fe	0.75	0.47	0.01	0.12	Orthoclase	24.9	20.5
Mn	0.05	0.03	0.00	0.01	Apatite	2.05	1.36
Mg	1.00	0.84	0.00	0.36	Chromite	0.02	0.02
Ca	0.18	0.58	0.06	3.81	Ilmenite	1.43	2.31
Na	0.01	0.04	0.88	0.34	Corundum	0.00	0.45
K	—	0.00	0.03	—			
P	0.00	0.00	0.00	3.01			
Total	4.01	4.01	4.99	7.65			
Wo	9.37	30.6					
En	51.8	44.7					
mg#	57.1	64.4			mg#	7.96	8.64
An			5.74		An	0.0	0.0
Ab			90.8				

[a] n.d. = not detected.

monly with lower anorthite content than plagioclase phenocrysts in the same clast) are intergrown with skeletal pyroxene and a glassy mesostasis (Fig. 2b). Several clasts have glassy feldspathic areas containing very fine crystallites, which may be more rapidly cooled versions of the intersertal-textured areas.

Only a few of the clasts in the population show the complete phase assemblage and range of textural features. Most appear to be unrepresentative samples of the complete assemblage. In addition, a significant number of the plagioclase mineral clasts ($n = 42$) in these polymict ureilites, along with two clasts consisting of feldspathic glass, have compositions similar to those of plagioclase in the polymineralic albitic clasts and probably also belong to this population. Type C1 feldspathic clasts identified by Ikeda et al. (2000) and Ikeda and Prinz (2001) have mineralogies that identify them as part of the albitic clast population (Fig. 4).

The common textural, mineralogical, and mineral compositional features of the albitic clasts suggest that they represent a common lithology. Mineral compositional trends among the clasts further support this interpretation, and show that the lithology they represent is most likely igneous. Figure 5a shows a plot of Fe/Mg vs. Fe/Mn (molar ratios) for pyroxenes in the albitic clasts compared to those in monomict olivine-pigeonite ureilites. Pyroxenes in olivine-pigeonite ureilites show a characteristic trend of constant Mn/Mg ratio (a linear trend passing through the origin), which indicates that ureilites are not related to one another by a progressive igneous process but rather by various degrees of reduction (carbon redox control, or smelting) due to derivation from a range of pressures/depths (Goodrich et al., 1987; Goodrich and Delaney, 2000). In contrast, pyroxenes in the albitic clasts show a trend of near-constant Fe/Mn ratio, typical of igneous fractionation (Goodrich and Delaney, 2000), over a range of Fe/Mg ratios much greater than that seen in olivine-pigeonite ureilites, and extending to much higher values. There is also a negative correlation, typical of igneous fractionation, between anorthite (An) content of plagioclase and Fe/Mg ratios of coexisting pyroxene (Fig. 6). These relationships suggest that the clasts are related to one another by fractional crystallization of a common melt.

3.2. Labradoritic Clasts

A smaller group of clasts ($n = 8$) is characterized by labradoritic plagioclase (An_{40-58}) in association with pyroxene, Si-rich glass, and in at least one case, ülvospinel. This lithology was found principally in DaG 665 and in one clast in EET 83309. A representative multi-phase clast is shown in Figure 7 and Table 4. The range of all plagioclase and pyroxene compositions in this population is shown in Figure 8.

Pyroxene grains are normally zoned or show signs of resorption and rimming with Ca-rich cores and Fe-rich rims (Fig. 7). Plagioclase occurs principally as masses of laths, interstitial to the pyroxenes. The mesostasis in these clasts is extremely

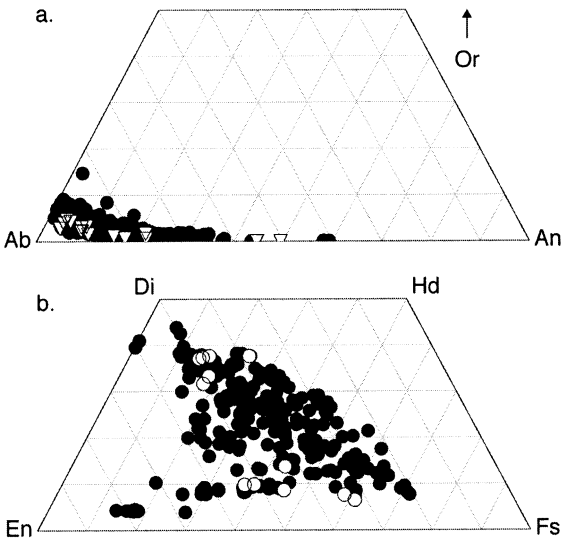

Fig. 4. Plagioclase and pyroxene compositions in albitic clasts (solid points = data from this paper; open points = data from Ikeda et al., 2000; Guan and Crozaz, 2001; Ikeda and Prinz, 2001). (a) Plagioclase ranges continuously through $An_{1-35}Ab_{93-41}Or_{0-14}$; (b) pyroxene shows both low-Ca and high-Ca fractionation trends.

silica-rich but not as enriched in incompatible elements as is the mesostasis in the albitic clasts (Table 4). Neither ilmenite nor chromite was observed in association with these clasts, but clast D8 has large, interstitial ülvospinel grains (Table 4). Some clasts are very fine-grained, made up of small (2–10 μm) plagioclase laths and interstitial, irregularly-shaped pyroxene. For one of the finest-grained clasts (DaG 665 E7), a bulk composition and normative mineralogy were determined (based on uncorrected defocused-beam analyses); the normative composition is 85% feldspar (An_{49}), 4% orthopyroxene (mg# = 64), 11% quartz, and minor apatite, ilmenite, and chromite. Fourteen single plagioclase grains (An_{40-60}) from all five meteorites may also be part of this population.

Mineral compositions and compositional trends in the labradoritic clasts suggest that they also represent a fractionated igneous lithology, but one that is different from the albitic clast lithology described above. Pyroxenes show a trend of near-constant Fe/Mn ratio (Fig. 5b) over a range of Fe/Mg values similar to those in the albitic clasts but at generally higher Fe/Mn. Furthermore, they show a correlation between An content of plagioclase and Fe/Mg ratios of coexisting pyroxenes (Fig. 6).

3.3. Olivine-Augite Feldspathic Clasts

Five feldspathic clasts contain olivine and augite as the only mafic minerals. In four clasts, olivine appears as euhedral, normally-zoned crystals in labradoritic plagioclase (An_{39-54}). In two of these four, augite is well developed ($Wo_{30-48}En_{33-54}Fs_{6-24}$) (Fig. 9; Table 5), and in the other two, pyroxene is feathery or skeletal (compositions could not be quantitatively determined because of the small crystal size). One additional clast (C24) has a distinctive texture (Fig. 10; Table 6), in which albitic plagioclase (An_9) poikilitically encloses distinct blebs of ferroan olivine (Fo_{59-64}) and augite ($Wo_{44}En_{43}Fs_{13}$).

Olivine compositions range from Fo_{58} to Fo_{89}, which is more ferroan than olivine in the olivine-pigeonite ureilites (Fo_{76-95}). Pyroxene compositions are also more ferroan (mg# = 60–90) than in olivine-pigeonite ureilites. Pyroxene and olivine occurring in the same clast have similar mg# to each other, indicating equilibrium. Mineral analyses from all five clasts are shown in Figure 11.

With the exception of clast C24, olivines in the olivine-augite feldspathic clasts have near-constant Fe/Mn ratio and appear to show a normal igneous fractionation trend (Fig. 5c), again suggesting that they represent a common melt.

3.4. Other Clasts

Calcic plagioclase (An_{75-98}) occurs as single mineral grains in the polymict ureilites examined in this study. We identified ten calcic plagioclase grains but were not able to positively identify any other mineral as occurring in conjunction with them.

We identified two single grains of anorthoclase in DaG 665 ($An_{0.1-0.2}Ab_{80.1-83.7}Or_{16.1-19.7}$). They are crystalline and internally homogeneous and we could not determine any other minerals with which they are definitely associated.

Many other polymineralic clasts contain plagioclase with a range of An content (Fig. 12) and pyroxene and/or olivine with compositions that differ from those of olivine-pigeonite ureilites in being more calcic and more ferroan (Fig. 12), but which nevertheless lie on the monomict ureilite Fe/Mg – Fe/Mn ratios trend (Fig. 5d). Because we cannot discern igneous trends among these clasts, we are not able to model their petrogenesis or determine whether they have a common source.

Four clasts have quench textures (Figs. 13a,b), consisting of skeletal to feathery mafic material in crystalline plagioclase. The plagioclase in each quench-textured clast has a constant composition but the An content varies widely among clasts (An_{33-80}), probably indicating that this texture is not correlated with any specific mineralogy but is simply an indicator of rapid cooling. A normative calculation based on the bulk composition of each clast yields the Fe/Mn and Fe/Mg ratios in normative pyroxene; on a plot similar to Figure 5, the quench-textured clast pyroxenes plot along the line defined by olivine-pigeonite ureilites. This relationship suggests that these clasts crystallized under carbon redox conditions rather than as a rapidly-cooled counterpart to the igneous lithologies described above.

Two clasts contain rimmed pyroxene crystals (Figs. 13c,d). In these clasts, the pigeonite at the center of the grains is indistinguishable from pigeonite in monomict ureilites, but there is an abrupt change to a distinct, Ca-rich augite in the rims. Both the cores and rims follow the monomict ureilite Fe/Mn-Fe/Mg trend, indicating the presence of carbon. A possible explanation for these clasts is that olivine-pigeonite ureilite clasts were incorporated into a feldspathic melt, either during impact mixing or by magma-wall rock interactions. The pyroxene crystals were partially digested in the melt and rimmed as crystallization proceeded.

In two clasts, normally-zoned olivine is the only well-developed mafic mineral, and many small olivine crystals occur (Fig. 14). The plagioclase groundmass is albitic (An_{21}), glassy, and nonstoichiometric, enriched in FeO (7.20 wt%), MgO (2.41 wt%), TiO_2 (0.50 wt%), and P_2O_5 (0.83 wt%). These two clasts very closely resemble clast E309-

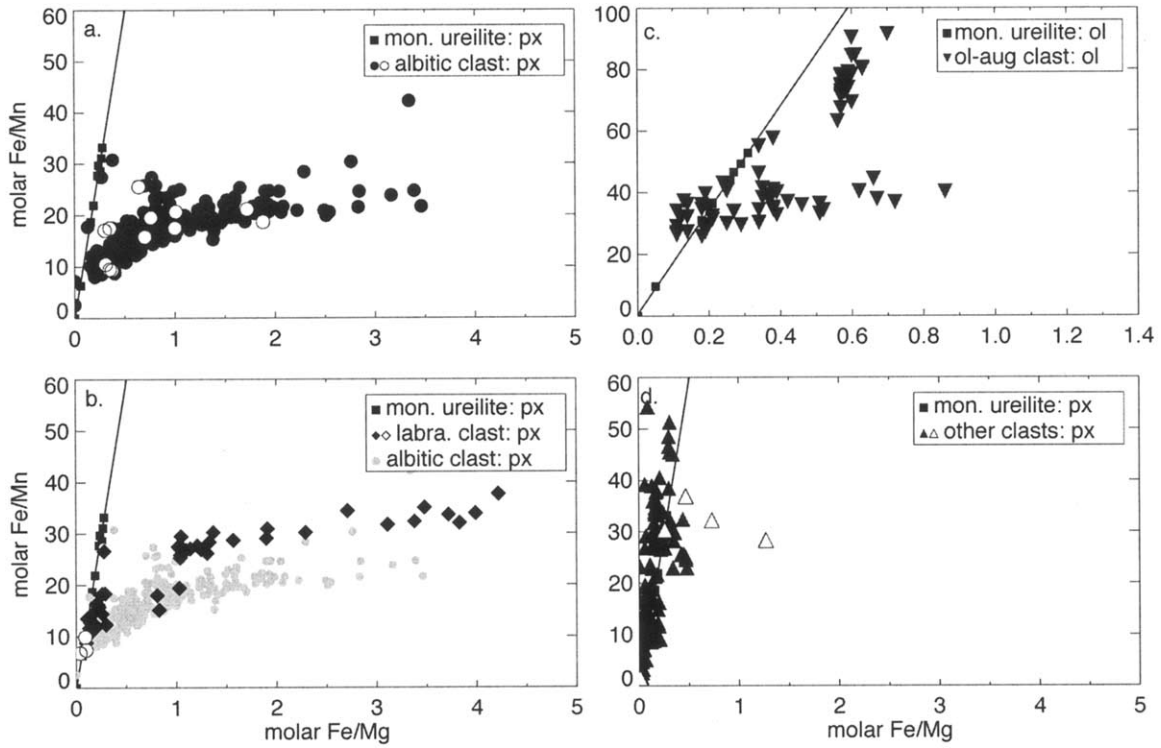

Fig. 5. Fe/Mg vs. Fe/Mn (molar ratios) for pyroxene and olivine in igneously-derived feldspathic clast populations in polymict ureilites (filled symbols = this paper, open symbols = data from Ikeda et al., 2000; Guan and Crozaz, 2001; Ikeda and Prinz, 2001) compared to olivine-pigeonite ureilites (Goodrich et al., 1987). Redox processes, such as those controlled by carbon, partition Fe between metal and silicate, while Mn and Mg are taken up solely by the mafic minerals. Monomict olivine-pigeonite ureilites, which contain carbon, contain olivine and pyroxene that lie along a linear trend of constant Mn/Mg, indicating carbon redox control without igneous fractionation. In contrast, mafic minerals in clasts derived from igneous processes in the absence of carbon show a near-constant Fe/Mn ratio over a wide range of Fe/Mg ratios. Igneous fractionation trends are visible in three populations of feldspathic clasts: (a) albitic clast pyroxene, (b) labradoritic clast pyroxene, and (c) olivine-augite clast olivine. Olivine compositions in clast C24, a distinctive, poikilitic olivine-augite clast, form a separate group in (c) at Fe/Mn = 60–90. Many other clasts also have igneous textures and mineralogies, but appear to have crystallized in the presence of carbon (d).

ML1 (Guan and Crozaz, 2001). Olivine compositions in these clasts, as well as those reported in Ikeda and Prinz (2001), fall on the carbon redox line and do not follow the fractionation trend defined by the olivine-augite clasts.

Several clasts (n = 8) contain laths or stripes of pyroxene ($Wo_{1-46}En_{48-92}Fs_{1-21}$) in plagioclase ($An_{13-83}$) (Fig. 15a,b). The pyroxene in these clasts is largely similar (mg# = 75–100) to that in olivine-pigeonite ureilites (mg# = 75–95). A few clasts (n = 2) have clastic textures and appear to be partially melted or plastically deformed breccias (Fig. 15c). One of these clasts is quite large (2 cm) and consists of irregular swathes of labradoritic plagioclase (An_{56}) around clasts of magnesian olivine (Fo_{83-89}) and augite ($Wo_{39}En_{56}Fs_5$). Areas of melt texture are common and randomly distributed (Fig. 15d).

4. DISCUSSION

4.1. Criteria for Pristinity

The main goal of this study was to identify feldspathic clasts representing lithologies that are not only indigenous to the UPB, but which are pristine (that is, generated by internal melting rather than impact melting). Though we believe that the albitic, labradoritic, and olivine-augite clasts represent primary igneous material from the UPB, other pristine products of UPB igneous activity may not be easily identified as such in a ureilitic regolith breccia. Pristine igneous products of the UPB may be expected to share several characteristics with impact-melted material that is common in such breccias.

Impact melt rocks form in the bottom of craters, where pressure-release melting of target material occurs (Melosh, 1989). The amount of melt produced in an impact event scales logarithmically with transient crater diameter (Cintala and Grieve, 1998) for a wide range of projectile compositions and impact velocities. Small craters produce small amounts of melt, which is rapidly quenched and found as glass soil coatings and in glassy breccias. The largest craters produce a thick melt sheet where a slow cooling rate facilitates crystallization in an igneous system, and which may be large enough to differentiate (e.g., Sudbury; Grieve et al., 1991; Therriault et al., 1999).

Because impact events cause target rocks to rapidly and completely melt, products of impact melting share many characteristics with igneous rocks produced by equilibrium melting processes. Historically, impact-melt rocks have been distinguished from other igneous rocks based on other distinctive

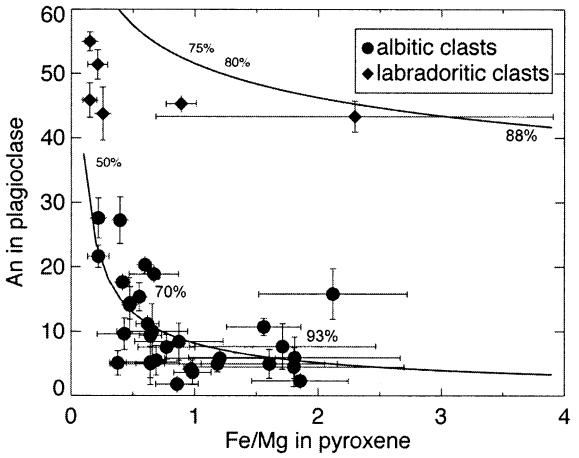

Fig. 6. Anorthite content (An) of plagioclase vs. Fe/Mg ratio (molar) of coexisting pyroxenes in albitic and labradoritic clasts in polymict ureilites. Error bars represent the range of observed compositions within each clast. The curves represent the fractional crystallization paths (as calculated by MAGPOX; Longhi, 1991) for each population; degree of crystallization (vol%) at various points is indicated. The albitic clast trend is fit by crystallization of a 6% partial melt of model ureilite precursor material that can produce the most magnesian olivine-pigeonite ureilites as residues (Fo_{92}; Goodrich, 1999), while labradoritic clast trend is fit by crystallization of a 5%–7% partial melt from a precursor material in equilibrium with a more ferroan olivine-pigeonite ureilite (Fo_{86}).

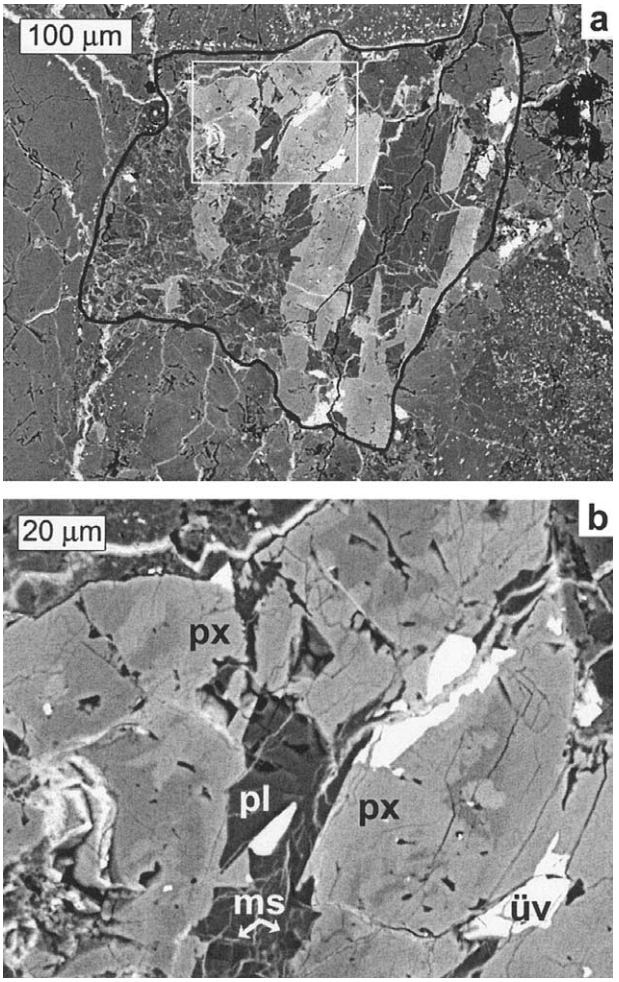

Fig. 7. Backscattered electron images of EET 83309 Clast D8, a labradoritic clast. (a) Clast is outlined in black, white box shows the area of the enlarged view; (b) large pyroxene laths (px) have irregular boundaries where Mg-rich cores show signs of resorption and are rimmed by more ferroan pyroxene. Pyroxene and small ülvospinel grains (üv) are set in a groundmass of labradoritic plagioclase (pl) and Si-rich mesostasis (ms).

features in the impact-melt rocks: evidence of extremely high pressures (such as shock-metamorphosed inclusions), unusual bulk chemical compositions, or chemical signatures from the projectile itself. However, these distinctions are not straightforward for rocks on the UPB.

Rapid cooling of impact-melted material typically produces glassy and quench-textured rocks, but if explosive volcanism occurred on the UPB as has been suggested (Warren and Kallemeyn, 1992; Scott et al., 1993), remnants of volcanism might also be glassy and quench-textured. Unique textures may arise in rocks as a result of rapid melting followed by cooling such as in impact melts, when the short-range order in the melt is not entirely destroyed by the melting event and minerals are able to nucleate and crystallize rapidly (Lofgren, 1983). For example, the "haystack" texture that arises from rapid plagioclase crystallization is seen in a few of the feldspathic clasts in this study, suggesting that they are impact melts. The small size of typical feldspathic clasts in polymict ureilites (<500 μm) makes it unlikely that they will contain inclusions of shocked or unmelted material.

Evidence of impact origin is commonly determined using geochemistry of breccias or melt rocks, even those without shock features. In particular, siderophile element enrichment has become a standard method for the identification of impact-generated or -reworked materials on differentiated bodies such as the Moon and the howardite-eucrite-diogenite parent body (Vesta). The separation of metal into the core during differentiation sequesters siderophile elements in the core and depletes them in the crust and mantle. Subsequent addition of chondritic material by impact is thus detectable by the increased abundance of siderophile elements in impact melt rocks or breccias. Impact melt rocks are the main carrier of meteoritic material in large terrestrial impact craters (Janssens et al., 1977; Grieve, 1978; Morgan and Wandless, 1983; Schmidt et al., 1997; Hart et al., 2002). Lunar highland rocks contain an excess of siderophile elements, which has been attributed to meteoritic influx after the formation of the lunar crust (Korotev, 1987), and impact-reworked material on the moon is distinguished by its high siderophile content (Korotev, 1987; Warren, 1993; Norman et al., 2001). However, metal separation and core formation probably did not occur on the UPB (Berkley and Jones, 1982; Goodrich et al., 1987). Siderophile element abundance in ureilites ranges from $0.02 \times$ CI – $2 \times$ CI (Mittlefehldt et al., 1998) and therefore contamination by chondritic impactors would not be not evident in the siderophile element content.

Another signature of impact origin of a rock is a bulk chemical or isotopic composition that matches the target materials (e.g., at Manicouagan; Floran et al., 1978). Impact melts from the L5 parent body (Shaw, Chico, Cat Mountain) are melted rocks retaining chondritic compositions and containing

Table 4. Representative mineral analyses in EET 83309 Clast D8, a labradoritic clast.[a]

Oxide (wt%)	Pyroxene (rim)	Pyroxene (core)	Plagioclase	Ülvospinel	Oxide (wt%)	Mesostasis
SiO_2	46.62	48.28	57.75	0.51	SiO_2	95.63
TiO_2	0.9	0.9	n.d.	32.6	TiO_2	0.3
Al_2O_3	0.47	2.12	26.86	1.31	Al_2O_3	2.60
Cr_2O_3	0.1	0.9	n.d.	1.1	Cr_2O_3	n.d.
FeO	37.86	22.43	0.74	63.67	FeO	0.47
MnO	1.17	0.88	0.00	0.66	MnO	n.d.
MgO	5.54	12.10	0.08	0.11	MgO	n.d.
CaO	7.12	12.09	9.07	0.24	CaO	0.34
Na_2O	0.07	0.14	6.40	n.d.	Na_2O	0.14
K_2O	n.a.	n.a.	0.4	n.d.	K_2O	n.d.
P_2O_5	n.a.	n.a.	n.d.	n.d.	P_2O_5	n.d.
Total	99.82	99.85	101.29	100.24	Total	99.47
Cations	(O_6)	(O_6)	(O_8)	(O_4)	Normative mineralogy (vol%)	
Si	1.94	1.89	2.57	0.02	Quartz	95.3
Ti	0.03	0.03	0.00	0.91	Anorthite	1.64
Al	0.02	0.10	1.41	0.06	Hypersthene	0.30
Cr	0.00	0.03	0.00	0.03	Albite	1.30
Fe	1.32	0.73	0.03	1.97	Orthoclase	0.00
Mn	0.04	0.03	0.00	0.02	Apatite	0.00
Mg	0.34	0.71	0.01	0.01	Chromite	0.00
Ca	0.32	0.51	0.43	0.01	Ilmenite	0.30
Na	0.01	0.01	0.55	—	Corundum	1.17
K	—	—	0.02	—		
P	—	—	0.00	—		
Total	4.02	4.03	5.01	3.03		
Wo	16.0	26.0				
En	17.4	36.2				
mg#	20.7	49.0			mg#	7.24
An			43.0		An	55.6
Ab			54.8			

[a] n.a. = not analyzed; n.d. = not detected.

shocked clasts of primitive material (Taylor et al., 1979; Bogard et al., 1995; Kring et al., 1996). When the target is unknown, impact melt rocks may be identified by having a bulk composition that cannot be derived by common igneous fractionation processes in reasonable starting materials, but is better matched by mixing of likely target materials (such as has been proposed for EETA79001; Mittlefehldt et al., 1999). The composition of UPB primary basalts is largely unconstrained, so we cannot necessarily use a rock composition derived from a total melt to distinguish between igneous fractionation and impact mixing. On the other hand, if a rock composition or mineral assemblage can be demonstrated to be produced by a low-to-intermediate degree of partial melting from a plausible precursor, then a magmatic origin for the rock may be argued.

One of the features of monomict ureilites that distinguishes them from other differentiated meteorites is that they have high carbon contents (up to ~5 wt%), and carbon redox reactions appear to have been the main control on their mafic silicate compositions. This is evidenced principally in their Fe/Mn-Fe/Mg systematics (Fig. 5). Carbon would be expected to have been equally abundant in melts related to these residues, and to have controlled their redox states during ascent to lower pressures. However, the main feldspathic clast populations identified in this study appear to represent melts that crystallized in the absence of carbon. This strongly suggests that they are not impact melts, because carbon is also ubiquitous in the polymict ureilites (which represent regolith material) and it is difficult to envision any target material in the UPB regolith devoid of carbon. We would expect that impact melts crystallized in this environment would have highly magnesian mafic minerals with constant Mn/Mg. Therefore, it seems inescapable that some primary melts generated on the UPB crystallized in the presence of little or no carbon.

4.2. Modeling of Sources of Igneous Populations

Because they exhibit normal igneous fractionation trends without carbon redox control, we believe that the albitic, labradoritic, and olivine-augite clasts are pristine products of igneous differentiation on the UPB. We therefore investigate models for their origin from plausible ureilitic partial melts and their relationships to the olivine-pigeonite ureilites.

4.2.1. Albitic clasts

The Fe/Mn-Fe/Mg trend shown by the albitic clasts (Fig. 5a) originates from compositions near to those of the most magnesian monomict ureilites, suggesting that the melt they represent may have been complementary to such residues. Model calculations indicate that this is, indeed, reasonable. Goodrich (1999) showed that precursor materials that can produce olivine-pigeonite assemblages as residues must have had superchondritic Ca/Al ratios (with chondritic or slightly subchondritic Al/Mg ratios) and low alkali con-

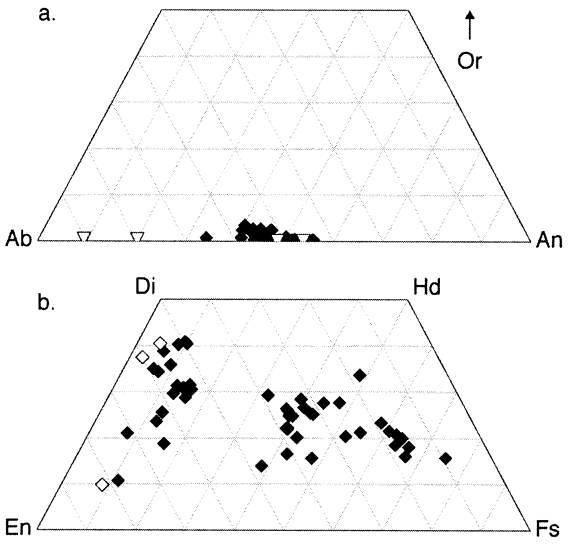

Fig. 8. Plagioclase and pyroxene compositions in labradoritic clasts (solid points = data from this paper; open points = data from Ikeda et al., 2000; Guan and Crozaz, 2001; Ikeda and Prinz, 2001). (a) Plagioclase ranges continuously through $An_{34-56}Ab_{44-65}Or_{0-3}$; (b) pyroxene shows a range of compositions from low- to high-Ca with normal fractionation trends.

tents similar to those in carbonaceous chondrites. The most magnesian olivine-pigeonite ureilites (Fo_{92}) require precursors with Ca/Al ~3.5 × CI. Starting with such a composition (Goodrich, 1999), we have taken melts produced at ~5% (the lower limit at which melts would be able to migrate from their source regions; L. Wilson, personal communication) to 25% (the point at which they are in equilibrium with the ureilite residues) melting, and calculated their fractional crystallization sequence (all calculations done with MAGPOX and MAGFOX; Longhi, 1991). Results show that although all melts produce a trend of An vs. Fe/Mg having the form of that shown by the albitic clasts, only the lowest degree melts will produce plagioclase compositions as albitic as those observed (Fig. 6). Higher Na contents in the starting materials would result in higher degree melts that could fractionate to the observed trend, but would produce olivine-orthopyroxene rather than olivine-pigeonite residues. Lower Al contents in the starting materials would have the same effect, but seem unlikely because plausible mechanisms for producing superchondritic Ca/Al ratios in the starting materials involve enrichment of Ca rather than loss of Al (Goodrich et al., 2002b). Furthermore, the predicted crystallization sequence for low-degree partial melts (plagioclase → intermediate and high-Ca pyroxenes → ilmenite + silica + phosphate) is consistent with the observed mineralogy, as well as the textures (occurrence of plagioclase as phenocrysts, and occurrence of silica and ilmenite only in the highly-fractionated glassy mesostases) of these clasts. These results suggest that the lithology represented by the population of albitic clasts in these polymict ureilites formed by extensive fractional crystallization of the earliest melt(s) of precursor materials from which the most magnesian ureilites were produced as residues.

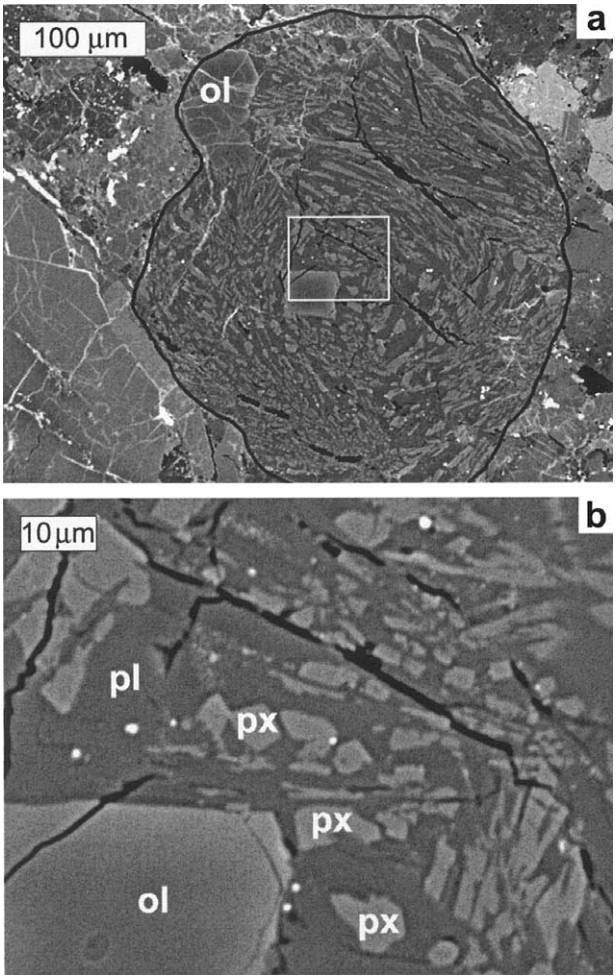

Fig. 9. Backscattered electron images of DaG 319 clast B38, an olivine-augite clast. (a) Clast is outlined in black, white box shows the area of the enlarged view; (b) plagioclase (pl) encloses a large, normally-zoned, euhedral olivine grain (ol) and skeletal pyroxene grains (px). The pyroxene grains have a range of compositions, but because of their small size, it was difficult to determine whether they are zoned or whether each grain has a different composition.

4.2.2. Labradoritic clasts

We attempted to fit the apparent igneous trend shown by pyroxene in the labradoritic clasts (Fig. 6) using several models. In the first model, we began with the same precursor material as that used for the albitic clasts, but increased the amount of partial melt extracted to 10%–20%. In the second model, we began with the material left after melt extraction to form the albitic clasts, and extracted a second batch of 5% melt from this residue composition. Neither model was able to produce plagioclase with An contents higher than ~40, and then only in equilibrium with more magnesian pyroxenes than those coexisting with An_{40} in the labradoritic clasts. Though higher degrees of partial melt increase the An number of plagioclase, plagioclase is fully in the melt fraction by ~10% melting. After this point, the An content of the plagioclase cannot change.

We then examined a starting composition that would be able to produce a more ferroan olivine-pigeonite ureilite (Fo_{86}) as a

Table 5. Representative mineral analyses in DaG 319 clast B38, an olivine-augite clast.[a]

Oxide (wt%)	Low-Mg Pyroxene	High-Mg Pyroxene	Low-Mg Olivine (rim)	High-Mg Olivine (core)	Plagioclase (glassy)
SiO_2	54.22	48.50	37.60	39.39	56.50
TiO_2	0.1	0.3	n.d.	n.d.	n.d.
Al_2O_3	2.17	6.37	0.20	n.d.	26.57
Cr_2O_3	0.9	3.3	0.3	0.6	0.1
NiO	n.a.	n.a.	0.04	n.a.	n.a.
FeO	9.62	3.16	22.98	9.93	0.78
MnO	0.8	0.3	0.7	0.3	0.1
MgO	18.11	15.49	37.90	49.43	1.32
CaO	13.60	20.91	0.34	0.27	9.53
Na_2O	0.28	0.43	n.d.	n.d.	6.37
K_2O	n.a.	n.a.	n.a.	n.a.	n.d.
P_2O_5	n.a.	n.a.	n.a.	n.a.	n.d.
Total	99.80	98.68	100.13	100.01	101.19
Cations	(O_6)	(O_6)	(O_8)	(O_8)	(O_8)
Si	1.98	1.80	1.97	1.94	2.52
Ti	0.00	0.01	—	—	—
Al	0.09	0.28	0.01	—	1.40
Cr	0.03	0.10	0.01	0.03	0.00
Ni	—	—	0.00	—	—
Fe	0.29	0.10	1.01	0.41	0.03
Mn	0.02	0.01	0.03	0.01	0.00
Mg	0.99	0.86	2.96	3.63	0.09
Ca	0.53	0.83	0.02	0.01	0.46
Na	0.02	0.03	—	—	0.55
K	—	—	—	—	0.00
P	—	—	—	—	—
Total	3.96	4.02	6.02	6.04	5.05
Wo	29.4	46.5			
En	54.4	48.0			
mg#	77.0	89.7	74.6	89.9	
An					45.2
Ab					54.6

[a] n.a. = not analyzed; n.d. = not detected.

residue, based on the observation that the Fe/Mn-Fe/Mg fractionation trend of the labradoritic clast pyroxenes (Fig. 5b) appears to intercept the olivine-pigeonite ureilite trend at a more ferroan composition than that of the albitic clast pyroxenes. This starting material has Ca/Al = 2 × CI (Goodrich, 1999), lower than the ratio in the albitic clast modeling. The fit shown in Figure 6 is achieved by fractional crystallization of a 5%–7% partial melt extracted from this starting material. The higher amount of Al in the melt (compared to that in the albitic clast model) increases the An content of the plagioclase, though the overall form of the fractional crystallization curve remains the same. Crystallization of this more ferroan partial melt produces a good fit to the overall trend, suggesting that the labradoritic clasts were produced by an episode of partial melting from deeper within the UPB than the albitic clasts.

4.2.3. Olivine-Augite clasts

The near-constant Fe/Mn ratio of olivine in the olivine-augite clasts (except C24) suggests that they represent a pristine ureilitic melt (Fig. 5c). This melt, however, cannot be modeled as complementary to the olivine-pigeonite ureilites, because in all such melts olivine is in reaction relationship with low-Ca pyroxene (Goodrich, 1999) and so it does not crystallize. However, melts having the crystallization sequence olivine + augite → plagioclase, consistent with the mineralogy and texture of clast B38 (Fig. 9), may have formed at depths greater than those at which the olivine-pigeonite ureilites formed on the UPB.

As discussed by Goodrich et al. (2002b), it is likely that the bulk UPB had an iron content similar to that of Allende (mg# ~62) if all iron was in the form of FeO. At pressures < ~100–125 bars, carbon redox reactions (smelting) resulted in reduction of some of the iron, hence generating the range of higher mg# values (~75–95) seen in the olivine-pigeonite ureilites (Berkley and Jones, 1982; Goodrich et al., 1987; Warren and Kallemeyn, 1992; Walker and Grove, 1993; Singletary and Grove, 2003b). However, at higher pressures (and magmatic temperatures), carbon redox reactions buffer mg# values lower than that of Allende, and so no smelting would have occurred. Under these conditions, ureilite precursor materials would lie in the olivine + augite stability field (Goodrich, 1999). Residues of ~20%–30% melting of such material would consist of olivine + augite, and complementary melts would crystallize olivine + augite, followed by plagioclase.

If these melts crystallized at depths near those at which they were generated, they would produce olivine and augite with more FeO-rich compositions (lower mg#) than those of the

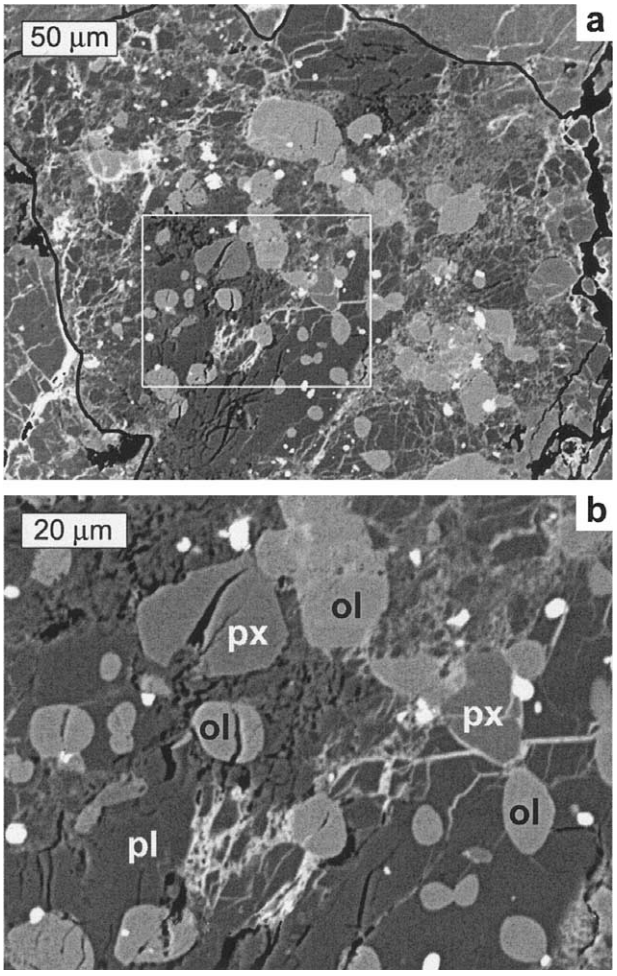

Fig. 10. Backscattered electron images of DaG 164 clast C24, an olivine-augite clast. (a) Clast is outlined in black, white box shows the area of the enlarged view; (b) crystalline, albitic plagioclase (pl) poikilitically encloses distinct blebs of unzoned olivine (ol) and pyroxene (px).

Table 6. Representative mineral analyses in DaG 164 Clast C24, an olivine-augite clast.[a]

Oxide (wt%)	Pyroxene	Olivine	Plagioclase
SiO_2	53.54	36.27	64.66
TiO_2	0.1	n.d	n.d
Al_2O_3	0.52	n.d	20.95
Cr_2O_3	0.2	n.d	0.1
NiO	n.a.	0.50	n.a.
FeO	8.34	31.81	1.27
MnO	0.16	0.42	0.18
MgO	15.12	30.63	0.02
CaO	21.03	0.10	1.95
Na_2O	0.75	n.d	9.91
K_2O	n.d	n.d	1.0
P_2O_5	0.0	0.1	0.1
Total	99.77	99.78	100.06
Cations	(O_6)	(O_8)	(O_8)
Si	1.99	2.00	2.87
Ti	0.00	—	—
Al	0.02	—	1.10
Cr	0.01	0.00	0.00
Ni	—	0.02	—
Fe	0.26	1.46	0.05
Mn	0.01	0.02	0.01
Mg	0.84	2.50	0.00
Ca	0.84	0.01	0.09
Na	0.05	—	0.85
K	—	—	0.06
P	0.00	0.00	0.00
Total	4.02	6.01	5.03
Wo	43.3		
En	43.3		
mg#	76.4	63.2	
An			9.27
Ab			85.2

[a] n.a. = not analyzed; n.d. = not detected.

olivine-pigeonite ureilites. However, if they rose to shallower depths (lower pressures), and contained carbon (which is likely), they would be reduced. Our calculations indicate that ~10%–12% partial melts, generated at pressures above the smelting pressure, could be reduced to mg# ~90 before they left the augite stability field. Such melts would then crystallize to an assemblage such as that seen in clast B38 (Fig. 9). Again, the normal zonation and constant Fe/Mn ratios of olivine and augite in these clasts can only be explained if carbon was absent during crystallization.

The assemblage seen in clast C24 (Fig. 10) is more difficult to explain. The ferroan compositions of its olivine and augite, and its relatively coarse-grained texture, suggest crystallization as a cumulate from a melt generated at depth. The Fe/Mn-Fe/Mg compositions of its olivine are distinct from those of the other olivine-augite clasts (Fig. 5c), and are consistent with such an origin: they plot near the monomict ureilite trend (but still at significantly higher Mn/Mg ratios), as expected for cumulus minerals (Goodrich and Delaney, 2000). However, its plagioclase is much more albitic than our models predict, unless it crystallized from a much later, more fractionated melt than the mafic minerals.

4.2.4. Anorthitic plagioclase

Single-grain anorthite clasts associated with FeO-rich olivine have been described in previous studies of polymict ureilites (e.g., population C4; Ikeda et al., 2000) and interpreted as Angra dos Reis (ADOR)-like clasts that were contributed by impactors (Prinz et al., 1986, 1987). Kita et al. (1999) showed that the oxygen isotopic composition of one such clast is similar to that of ADOR, supporting its foreign origin. Nevertheless, our calculations indicate that it is possible that some anorthite-rich plagioclase clasts are indigenous to the UPB. As discussed above, precursor materials with very high Ca/Al ratios (e.g., 3.5 × CI) lose plagioclase at low degrees of melting (~10% batch), and produce only albite-rich plagioclase. Fractional melting results in increased anorthite contents, but does not have a significant effect when total degree of melting is so small. However, precursor materials with Ca/Al = 2 × CI, such as those used to model the labradoritic clasts, retain plagioclase to higher degrees of melting (i.e., ~18% batch) and produce more anorthite-rich plagioclase. Repeated extraction of partial melts from such materials (incremental batch melting) can lead to melts that crystallize plagioclase with anorthite contents >90. This result is consistent with conclusions based on trace and

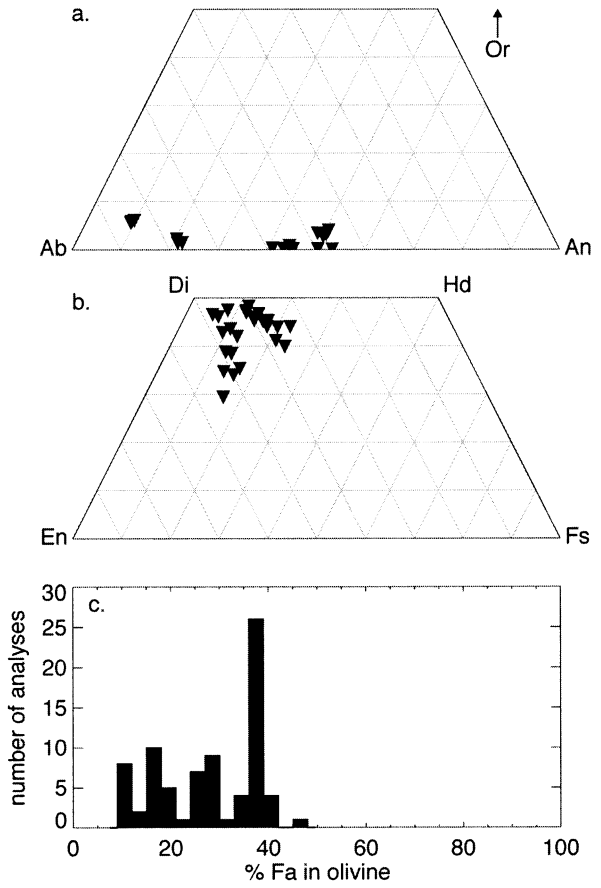

Fig. 11. Mineral compositions in olivine-augite clasts. (a) Plagioclase compositions are constant within each clast but the range among clasts is wide ($An_{9-54}Ab_{42-85}Or_{0-6}$); (b) pyroxene is high-Wo augite; (c) olivine ranges from Fo_{53} to Fo_{88}.

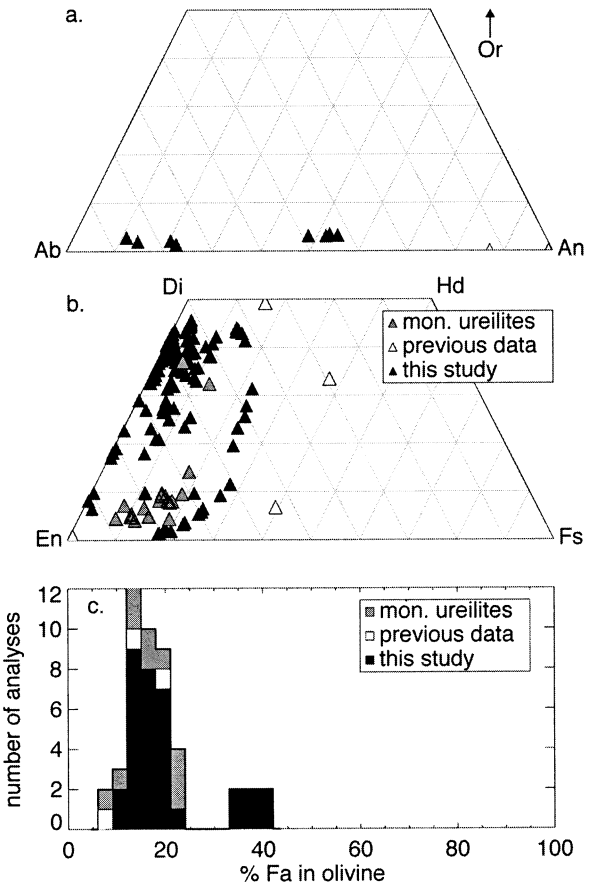

Fig. 12. Mineral compositions in feldspathic clasts not belonging to igneous trends. (a) Plagioclase ranges through $An_{9-91}Ab_{9-86}Or_{0-6}$; (b) pyroxene shows a wide range of mostly high-magnesian compositions; (c) olivine compositions form two groups, some similar to olivine-pigeonite ureilites (Fo_{75-95}) and some with more magnesian compositions (Fo_{60-64}).

rare earth element modeling (Guan and Crozaz, 2001), that the high-Ca and low-Ca plagioclase in polymict ureilites cannot be derived from a common magma source.

4.3. Implications for UPB Igneous History

The most likely environment in which carbon-poor melts could have been generated is in the shallowest (lowest-pressure) source regions, where most of the original carbon budget of the precursor material had already been consumed by reduction. The albitic clast trend in Figure 5 originates from the most magnesian range of the olivine-pigeonite ureilite trend and our model calculations suggest that these melts are indeed related to the most magnesian ureilite residues. These residues are derived from the shallowest depths on the parent body (~10–25 bars pressure; Warren and Kallemeyn, 1992; Walker and Grove, 1993; Sinha et al., 1997), and experienced the highest degree of reduction. Assuming, then, that the original carbon content of the parent body was relatively constant, the most magnesian ureilites would have had the lowest carbon contents (evidence for this has recently been found by Singletary and Grove, 2002, 2003b), and melts related to this material are the most likely (compared to melts related to more ferroan ureilite residues) to have been carbon-free. This may explain why the albitic clasts are the most abundant feldspathic materials (found so far) in polymict ureilites that show a normal fractionation pattern. In addition, since the high carbon contents (leading to high CO_2 contents) of ureilite melts are thought to have resulted in explosive eruption and loss from the parent body (Wilson and Keil, 1991; Scott et al., 1993), thus accounting for the absence of basaltic ureilites in the meteorite record and the scarcity of feldspathic material in polymict ureilites, the carbon-free (or low-carbon) melts related to the most magnesian ureilites are those most likely to have been preserved.

Our modeling suggests that the labradoritic clasts (which also appear to have crystallized in the absence of carbon) represent a partial melt that was derived from a deeper location in the ureilite parent body than the albitic clasts and was complementary to more ferroan olivine-pigeonite residues. This melt would have originally been less reduced than that which produced the albitic clasts. Its ascent, however, must have resulted in reduction (because, as discussed above, it is likely to have contained carbon), until the point at which its carbon was completely consumed. Early crystallization products of this melt, while carbon was still present, might not be recognized as such using the criteria applied in this

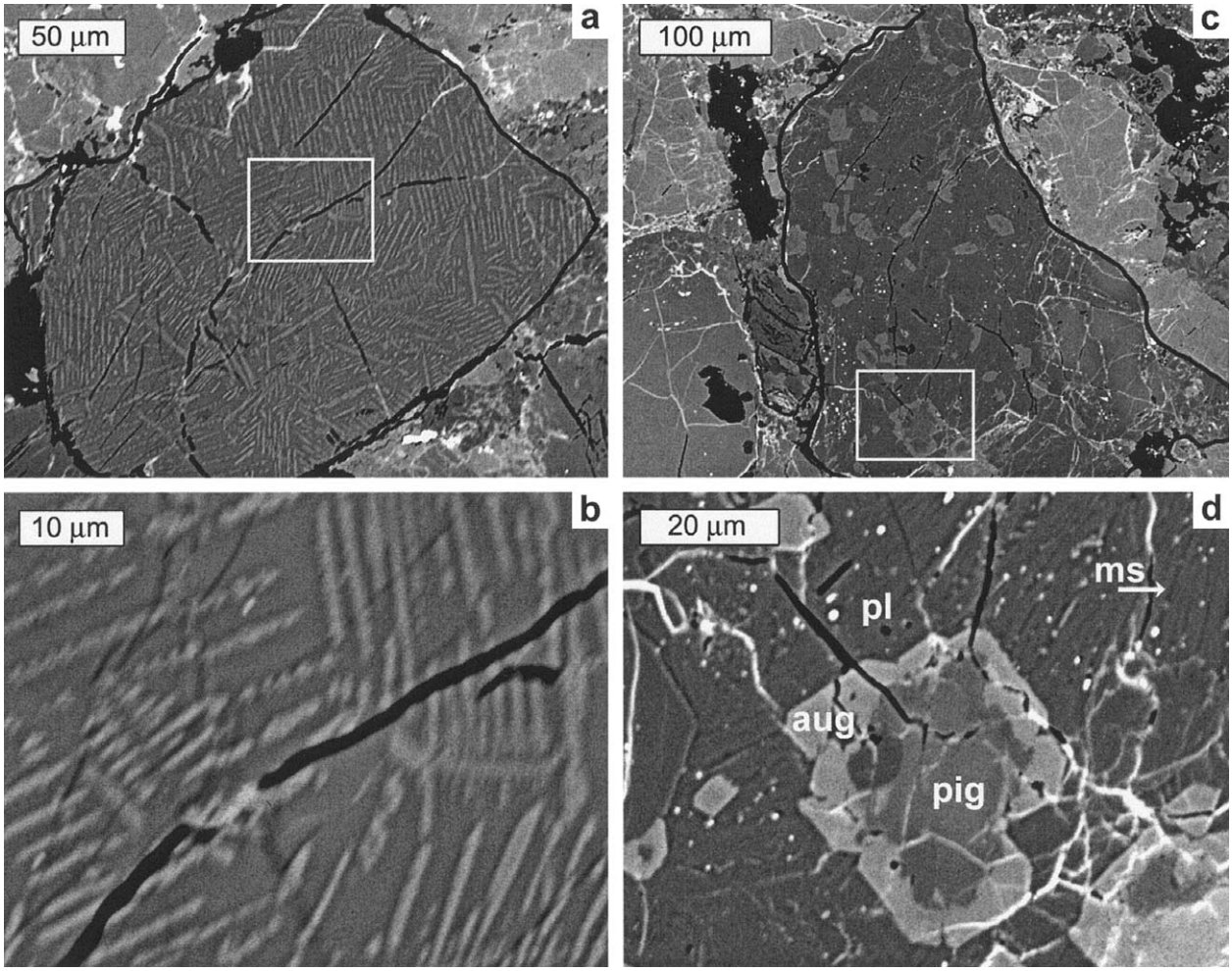

Fig. 13. Backscattered electron images of (a) DaG 319 Clast B33 (outlined in black), a pilotaxitic clast; white box shows the area of the enlarged view; (b) very finely skeletal mafic minerals are set in crystalline plagioclase (An_{41}). (c) DaG 319 Clast B23 (outlined in black) containing euhedral pyroxene grains; white box shows the area of the enlarged view; (d) larger pyroxene grains have partially resorbed pigeonite cores (pig; $Wo_1En_{92}Fs_7$) and euhedral augite rims (aug; $Wo_{34}En_{65}Fs_1$). The groundmass consists of plagioclase laths (pl; An_{14}) and mesostasis (ms).

work, and it is conceivable that some of the feldspathic clasts that plot along the monomict ureilite Fe/Mn-Fe/Mg trend (Fig. 5d) are actually such products and belong to the labradoritic clast population. This suggests that our modeling of the labradoritic population may not be strictly correct. The original melt may have been generated from more ferroan source material and at higher degrees of melting than used in our model. If melt extraction was an incremental (rather than completely batch) process, this might also explain the lack of extreme incompatible-element enrichment in the labradoritic clasts.

Our modeling further suggests that the olivine-augite feldspathic clasts represent melts that could only have been derived from even deeper source regions than those represented by the olivine-pigeonite ureilites ($P > \sim 100–125$ bars), in a region where smelting was suppressed and mafic mineral compositions were more ferroan than those in the olivine-pigeonite ureilites. Again, ascent of these melts would lead to reduction, and consumption of carbon. Thus, we suggest that all basaltic melts produced on the UPB, regardless of their depth of derivation, would have become highly reduced during ascent, but that due to consumption of most of their carbon in this process their later stages of crystallization were characterized by lack of carbon redox control and normal igneous fractionation trends such as those seen in Figures 5 and 6.

We observed many feldspathic clasts that cannot be identified as belonging to any of the three populations defined in this study. The majority of these clasts have igneous textures and contains olivine and/or pyroxene whose Fe/Mn ratios were controlled by carbon redox conditions (Fig. 5d). Their genesis is thus difficult to model based on major element analyses and mineral chemistry. However, from the argument just presented, it is clear that they could represent early products of ureilitic melts, which crystallized before carbon was completely consumed. It is also possible that some of them are impact melt products, where the target rocks included carbon-bearing monomict ureilite-like material. Impact melting of a polymict ureilite (which may be typical of the UPB regolith) would yield a melt containing <2% feldspathic material. However, the typical feldspathic clast contains >50% modal plagioclase. Therefore, impact-melting scenarios would be obligated to

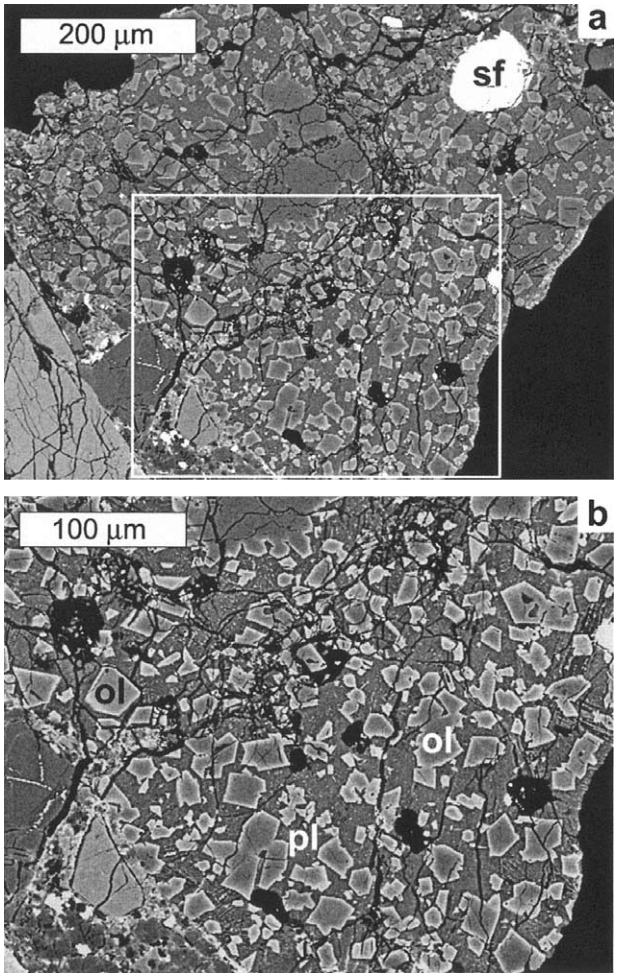

Fig. 14. Backscattered electron images of DaG 165 clast 24. (a) Euhedral olivine crystals in glassy plagioclase; large white grain is Fe-sulfide (qualitative identification by energy-dispersive system (EDS) spectral analysis); white box shows the enlarged view; (b) euhedral olivine grains (ol) are normally zoned (core Fo_{88}; rim Fo_{76}), plagioclase groundmass (pl; An_{40}) is nonstoichiometric and contains crystallites.

explain the presence of a substantial feldspathic component in the target materials. If most melts were lost due to explosive volcanism (Scott et al., 1993), it seems unlikely that substantial volumes of basalt were ever present as surface flows on the UPB. Thus, we are inclined to believe that the majority of feldspathic clasts in polymict ureilites represent pristine basaltic lithologies.

Finally, our arguments lead to the conclusion that melt extraction on the UPB was a fractional (or incremental) process. All of our models require either low- or intermediate-degree melts, rather than the 25%–30% melts that would be generated by a batch process. Additionally, fractional melting is required to explain the genesis of the very anorthite-rich plagioclase clasts observed. This conclusion seems reasonable, as fractional extraction of melts (in thin veins or dikes) is more consistent with preservation of heterogeneous oxygen isotopic compositions in the residues than is production and movement of large batches of melt.

The timing of this melt extraction is constrained by age data that have been obtained from some feldspathic clasts in polymict ureilites. Two highly-fractionated clasts belonging to the albitic population (clast B1 from DaG 319, shown in Fig. 3, and clast 19 from DaG 165) have a well-defined ^{53}Mn-^{53}Cr age (determined from their FeO- and MnO-rich glass phase) of 4.5 ± 0.4 Ma before the angrites, yielding a calculated absolute age of 4.562 Ga (Goodrich et al., 2002a). This age is similar to that of the oldest eucrites, and thus demonstrates that melting on the UPB began very early in the history of the solar system. A Pb-Pb age (4.559 ± 28 Ga) consistent with this was obtained from apatite in two albitic clasts from DaG 319 (Kita et al., 2002). In addition, ^{26}Al-^{26}Mg measurements of a diverse suite of plagioclase-bearing clasts (An contents ranging from 2 to 96) in DaG 319 show clear excesses of ^{26}Mg and an initial $^{26}Al/^{27}Al$ value corresponding to $\sim$5 Ma after formation of CAIs (Kita et al., 2003), thus implicating ^{26}Al as the heat source for partial melting on the UPB. If ^{26}Al was the heat source for partial melting, parent-body thermal models (Grimm and McSween, 1989; Cohen and Coker, 2000) suggest that the deepest regions were heated first, and thus the olivine-augite clasts are predicted to be the oldest, with the labradoritic clasts and albitic clasts being progressively younger. Studies linking the ^{53}Mn-^{53}Cr system to the ^{26}Al-^{26}Mg system for these clasts are needed to further constrain the timing and duration of melting on the UPB. A short time scale for igneous processing is consistent with the conclusion of this study that melt extraction was fractional, and with the requirement that primitive chemical and isotopic signatures be preserved.

5. SUMMARY

We characterized the mineralogy, textures, and mineral compositions of 171 feldspathic clasts in five polymict ureilites. Based on this characterization, we have identified three populations of clasts, each of which appears to represent a common igneous lithology and shows normal igneous fractionation trends. Consideration of criteria for pristinity suggests that the melts represented by these three populations are indigenous products of igneous differentiation on the ureilite parent body, rather than impact melts.

The largest population is characterized by albitic plagioclase, in association with pyroxenes, phosphates, ilmenite, silica, and incompatible-element enriched glass. Partial melting and fractional crystallization calculations suggest that it formed by extensive fractional crystallization of the earliest melt(s) of precursor materials from which the most magnesian olivine-pigeonite ureilites were produced as residues. A less abundant population is characterized by more calcic (labradoritic) plagioclase, in association principally with pyroxenes. Calculations suggest that it formed from melts complementary to more ferroan olivine-pigeonite monomict ureilites, and derived from deeper in the UPB interior, than the albitic population. The third population that was identified is characterized by olivine and augite, in association with plagioclase of intermediate composition. Our modeling suggests that it represents a melt (or melts) derived from greater depths in the UPB than the olivine-pigeonite ureilites.

Many other feldspathic clasts cannot be positively associated with any of these three populations, because their mafic mineral

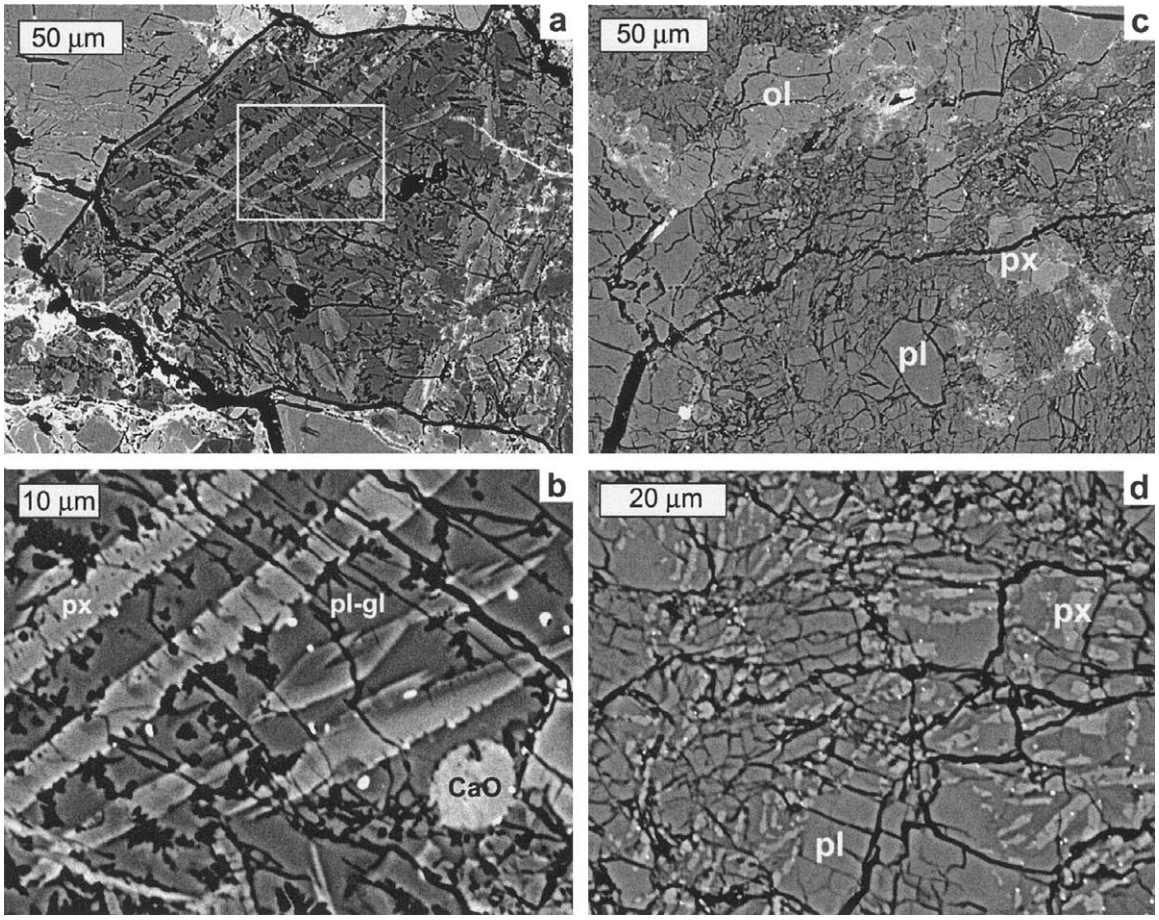

Fig. 15. Backscattered electron images of (a) DaG 665 clast E30 (outlined in black); white box shows the enlarged view; (b) pyroxene (px; $Wo_{8-29}En_{92-71}Fs_{0-3}$) occurs as laths in glassy plagioclase (pl-gl; An_{15-25}); small round grain is CaO (qualitative identification by energy-dispersive system (EDS) spectral analysis). (c) DaG 665 clast E50 (2 cm clast is much larger than area shown) appears to be a heated and/or deformed breccia, containing chunks of olivine (ol; Fo_{83-89}), augite (px; $Wo_{39}En_{56}Fs_5$), plagioclase (pl; An_{56}), and areas with melted textures. A typical melt texture is shown in (d), where skeletal pyroxene (px) occurs in plagioclase (pl).

compositions exhibit carbon redox control rather than igneous fractionation trends. However, we argue that early crystallization of all basaltic melts produced on the UPB may have been controlled by carbon redox reactions, and it is likely that many of these clasts are indeed pristine. Normal igneous fractionation trends would have been produced only in the later stages of crystallization, when carbon had been exhausted due to reduction during ascent. Therefore, late, highly-fractionated melts are the most readily identified among the feldspathic clasts of polymict ureilites.

Partial melting on the ureilite parent body was a fractional (or incremental), rather than batch, process. Melts were produced early in UPB history, and were most likely extracted rapidly, thus preserving primitive chemical and oxygen isotopic signatures in the residues.

Acknowledgments—We are grateful to the following for loan of samples in this study: A. Bischoff at the University of Münster for DaG 164 and 165; J. Zipfel at Max-Planck-Institut für Chemie for DaG 319; L. Folco at the Museo Nazionale dell'Antartide for DaG 665; and R. C. Greenwood at the Open University for FRO 93008. We thank N. Kita and I. Hutcheon for insightful discussions and two anonymous reviewers helped strengthen the manuscript. This study made use of the NASA Astrophysics Data System. This work was supported by NASA Cosmochemistry grant NAG 5-11591 to K. Keil and is HIGP publication 1297 and SOEST publication 6213.

Associate editor: C. Koeberl

REFERENCES

Berkley J. L. and Jones J. H. (1982) Primary igneous carbon in ureilites: Petrological implications. *J. Geophys. Res.* **87,** A353–A364.

Bogard D. D., Garrison D. H., Norman M., Scott E. R. D., and Keil K. (1995) ^{39}Ar-^{40}Ar age and petrology of Chico: Large-scale impact melting on the L chondrite parent body. *Geochim. Cosmochim. Acta* **59,** 1383–1399.

Cintala M. J. and Grieve R. A. F. (1998) Scaling impact melting and crater dimensions: Implications for the lunar cratering record. *Meteorit. Planet. Sci.* **33,** 889–912.

Cohen B. A. and Coker R. F. (2000) Modeling of liquid water on CM meteorite parent bodies and implications for amino acid racemization. *Icarus* **145,** 369–381.

Fioretti A. M. and Goodrich C. A. (2001) A contact between an olivine-pigeonite lithology and an olivine-augite-orthopyroxene li-

thology in ureilite FRO 93008: Dashed hopes? (abstract). *Meteorit. Planet. Sci.* **36,** A58.

Floran R. J., Grieve R. A. F., Phinney W. C., Warner J. L., Simonds C. H., Blanchard D. P., and Dence M. R. (1978) Manicouagan Impact Melt, Quebec, 1. Stratigraphy, petrology and chemistry. *J. Geophys. Res.* **83,** 2737–2759.

Goodrich C. A. (1992) Ureilites: A critical review. *Meteorit. Planet. Sci.* **27,** 327–352.

Goodrich C. A. (1999) Are ureilites residues from partial melting of chondritic material? The answer from MAGPOX. *Meteorit. Planet. Sci.* **34,** 109–119.

Goodrich C. A., Jones J. H., and Berkley J. L. (1987) Origin and evolution of the ureilite parent magmas; multi-stage igneous activity on a large parent body. *Geochim. Cosmochim. Acta* **51,** 2255–2273.

Goodrich C. A. and Delaney J. S. (2000) Fe/Mg-Fe/Mn relations of meteorites and primary heterogeneity of primitive achondrite parent bodies. *Geochim. Cosmochim. Acta* **64,** 149–160.

Goodrich C. A. and Keil K. (2002) Feldspathic and other unusual clasts in polymict ureilite DaG 165. *Lunar Planet. Sci.* **33,** 1777.

Goodrich C. A., Hutcheon I. D., and Keil K. (2002a) ^{53}Mn-^{53}Cr age of a highly-evolved, igneous lithology in polymict ureilite DaG 165. *Meteorit. Planet. Sci.* **37,** A54.

Goodrich C. A., Krot A. N., Scott E. R. D., Taylor G. J., Fioretti A. M., and Keil K. (2002b) Formation and evolution of the ureilite parent body and its offspring. *Lunar Planet. Sci.* **33,** 1379.

Grieve R. A. F. (1978) Meteoritic component and impact melt composition at the Lac a l'Eau Claire/Clearwater impact structures, Quebec. *Geochim. Cosmochim. Acta* **42,** 429–431.

Grieve R. A. F., Stoeffler D., and Deutsch A. (1991) The Sudbury structure—Controversial or misunderstood? *J. Geophys. Res.* **96,** 22753–22764.

Grimm R. E. and McSween H. Y.Jr. (1989) Water and the thermal evolution of carbonaceous chondrite parent bodies. *Icarus* **82,** 244–280.

Grossman J. N. (1997) The Meteoritical Bulletin, No. 81. *Meteorit. Planet. Sci.* **32,** A159–A166.

Grossman J. N. (1998) The Meteoritical Bulletin, No. 82. *Meteorit. Planet. Sci.* **33,** A221–A239.

Grossman J. N. and Zipfel J. (2001) The Meteoritical Bulletin, No. 85. *Meteorit. Planet. Sci.* **36,** A293–A322.

Guan Y. and Crozaz G. (2001) Microdistributions and petrogenetic implications of rare earth elements in polymict ureilites. *Meteorit. Planet. Sci.* **36,** 1039–1056.

Guan Y. and Leshin L. A. (2001) Oxygen isotopes of mineral and lithic clasts in the polymict ureilite EET 83309: An ion microprobe study (abstract). *Meteorit. Planet. Sci.* **36,** A74.

Hart R. J., Cloete M., McDonald I., Carlson R. W., and Andreoli M. A. G. (2002) Siderophile-rich inclusions from the Morokweng impact melt sheet, South Africa: Possible fragments of a chondritic meteorite. *Earth Planet. Sci. Lett.* **198,** 49–62.

Hicks T. L., Taylor G. J., Fagan T. J., Krot A. N., and Keil K. (2002) Automated mapping of meteorite thin sections using image processing software. *Lunar Planet. Sci.* **33,** 1055.

Ikeda Y., Prinz M., and Nehru C. E. (2000) Lithic and mineral clasts in the Dar Al Gani (DAG) 319 polymict ureilite. *Antarctic Meteor. Res.* **13,** 177–221.

Ikeda Y. and Prinz M. (2001) Magmatic inclusions and felsic clasts in the Dar al Gani 319 polymict ureilite. *Meteorit. Planet. Sci.* **36,** 481–499.

Janssens M.-J., Hertogen J., Takahashi H., Anders E., and Lambert P. (1977) Rochechouart meteorite crater—Identification of projectile. *J. Geophys. Res.* **82,** 750–758.

Kita N. T., Ikeda Y., Prinz M., Nehru C. E., Weisberg M. K., Morishita Y., and Togashi S. (1999) In-situ SIMS oxygen isotopic analyses of clasts from DaG 319 polymict ureilite. In *Symposium on Antarctic Meteorites*, Vol. 24, pp. 72–74. Tokyo, National Institute of Polar Research.

Kita N. T., Liu Y. Z., Ikeda Y., Prinz M., and Morishita Y. (2000) Identification of a variety of clasts in the Dar al Gani 319 polymict ureilite using secondary ion mass spectrometer oxygen-isotopic analyses (abstract). *Meteorit. Planet. Sci.* **35,** A88–A89.

Kita N. T., Ikeda Y., and Morishita Y. (2002) The old Pb-Pb age of apatite in felsic clast of polymict ureilite DaG 319 (abstract). *Meteorit. Planet. Sci.* **37,** A79.

Kita N. T., Ikeda Y., Shimoda H., Morishita Y., and Togashi S. (2003) Timing of basaltic volcanism in ureilite parentbody inferred from the ^{26}Al ages of plagioclase-bearing clasts in Dag-319 polymict ureilite. *Lunar Planet. Sci.* **34,** 1557.

Korotev R. L. (1987) The meteorite component of Apollo 16 noritic impact melt breccias. *J. Geophys. Res.* **92**, E491–E512.

Kring D. A., Swindle T. D., Britt D. T., and Grier J. A. (1996) Cat Mountain: A meteoritic sample of an impact-melted asteroid regolith. *J. Geophys. Res.* **101,** 29353–29372.

Lofgren G. E. (1983) Effect of heterogeneous nucleation on basaltic textures: A dynamic crystallization study. *J. Petrol.* **24,** 229–255.

Longhi J. (1991) Origin of picritic green glass magmas by polybaric fractional fusion. *Lunar Planet. Sci.* **22,** 343–353.

Melosh H. J. (1989) *Impact Cratering: A Geologic Process.* Oxford University Press.

Mittlefehldt D. W., McCoy T. J., Goodrich C. A., and Kracher A. (1998) Non-chondritic meteorites from asteroidal bodies. In *Planetary Materials*, Vol. 36 (ed. J. J. Papike), pp. 4-1 to 4-195. Mineralogical Society of America.

Mittlefehldt D. W., Lindstrom D. J., Lindstrom M. M., and Martinez R. R. (1999) An impact melt origin for Lithology A of Martian meteorite EETA79001. *Meteorit. Planet. Sci.* **34,** 357–367.

Morgan J. W. and Wandless G. A. (1983) Strangways Crater, Northern Territory, Australia: Siderophile element enrichment and lithophile element fractionation. *J. Geophys. Res.* **88,** A819–A829.

Norman M. D., Bennett V. C., and Ryder G. (2001) Highly siderophile (Re-PGE) and lithophile element geochemistry of Apollo 17 LKFM impact melts. *Lunar Planet. Sci.* **32,** 1418.

Pouchou J. L., Pichoir F. (1985) "PAP" $\phi(\rho Z)$ procedure for improved quantitative microanalysis. In *Microbeam Analysis—1985* (ed. J. T. Armstrong), pp. 104–106. San Francisco Press.

Prinz M., Weisberg M. K., Nehru C. E., and Delaney J. S. (1986) North Haig and Nilpena: Paired polymict ureilites with Angra dos Reis–related and other clasts. *Lunar Planet. Sci.* **17,** 681–682.

Prinz M., Weisberg M. K., Nehru C. E., and Delaney J. S. (1987) EET 83309, a polymict ureilite: Recognition of a new group. *Lunar Planet. Sci.* **17,** 802–803.

Satterwhite C. and Lindstrom M. (1998) *Antarctic Meteorite Newsletter* **21**.

Schmidt G., Palme H., and Kratz K. (1997) Highly siderophile elements (Re, Os, Ir, Ru, Rh, Pd, Au) in impact melts from three European impact craters (Saaksjarvi, Mien and Dellen): Clues to the nature of the impacting bodies. *Geochim. Cosmochim. Acta* **61,** 2977–2987.

Scott E. R. D., Taylor G. J., and Keil K. (1993) Origin of ureilite meteorites and implications for planetary accretion. *Geophys. Res. Lett.* **20,** 415–418.

Singletary S. J. and Grove T. L. (2002) Experimental constraints on the genesis of the olivine-pigeonite bearing ureilites. *Lunar Planet. Sci.* **33,** 1382.

Singletary S. J. and Grove T. L. (2003a) Early petrologic processes on the ureilite parent body. *Meteorit. Planet. Sci.* **38,** 95–108.

Singletary S. J. and Grove T. L. (2003b) Experimental investigations of ureilite petrogenesis: Relationships between mg# and smelting extent. *Lunar Planet. Sci.* **34,** 1192.

Sinha S. K., Sack R. O., and Lipschutz M. E. (1997) Ureilite meteorites: Equilibration temperatures and smelting reactions. *Geochim. Cosmochim. Acta* **61,** 4325–4242.

Smith C. L., Wright I. P., Franchi I. A., and Grady M. M. (2000) A statistical analysis of mineralogical data from Frontier Mountain ureilites (abstract). *Meteorit. Planet. Sci.* **35,** A150.

Taylor G. J., Keil K., Berkley J. L., Lange D. E., Fodor R. V., and Fruland R. M. (1979) The Shaw meteorite—History of a chondrite consisting of impact-melted and metamorphic lithologies. *Geochim. Cosmochim. Acta* **43,** 323–337.

Therriault A. M., Fowler A. D., and Grieve R. A. F. (1999) The Sudbury Igneous Complex: Mineralogy and petrology of a differentiated impact melt sheet. *Lunar Planet. Sci.* **30,** 1801.

Walker D. and Grove T. (1993) Ureilite smelting. *Meteoritics* **28,** 629–636.

Warren P. H. (1993) Chemistry, petrology and physics of lunar meteorite launch events. *Meteoritics* **28,** 45519.

Warren P. H. and Kallemeyn G. W. (1989) Geochemistry of polymict ureilite EET83309 and a partially-disruptive impact model for ureilite origin. *Meteoritics* **24,** 233–246.

Warren P. H. and Kallemeyn G. W. (1991) Geochemistry of unique achondrite MAC88177: Comparison with polymict ureilite EET87720 and "normal" ureilites. *Lunar Planet. Sci.* **22,** 1467–1468.

Warren P. H. and Kallemeyn G. W. (1992) Explosive volcanism and the graphite-oxygen fugacity buffer on the parent asteroid(s) of the ureilite meteorites. *Icarus* **100,** 110–126.

Wilson L. and Keil K. (1991) Consequences of explosive eruptions on small solar system bodies—The case of the missing basalts on the aubrite parent body. *Earth Planet. Sci. Lett.* **104,** 505–512.